JGS
Journal of the Geological Society

Research article

Published Online First

doi:10.1144/jgs2014-112

Contrasting mechanisms for crustal sulphur contamination of mafic magma: evidence from dyke and sill complexes from the British Palaeogene Igneous Province

Hannah S. R. Hughes[1,2*], Adrian J. Boyce[3], Iain McDonald[1], Brett Davidheiser-Kroll[3], David A. Holwell[4], Alison McDonald[3] & Anthony Oldroyd[1]

[1] School of Earth and Ocean Sciences, Cardiff University, Park Place, Cardiff CF10 3AT, UK
[2] Present address: School of Geosciences, University of Witwatersrand, PVT Bag 3, Wits 2050, Johannesburg, South Africa
[3] Scottish Universities Environment Research Centre, Rankine Avenue, East Kilbride, Glasgow G75 0QF, UK
[4] Department of Geology, University of Leicester, University Road, Leicester LE1 7RH, UK
* Correspondence: hannah.hughes@wits.ac.za

Abstract: The addition of crustal sulphur to magma can trigger sulphide saturation, a process fundamental to the development of some Ni–Cu–PGE deposits. In the British Palaeogene Igneous Province, mafic and ultramafic magmas intrude a thick sedimentary sequence offering opportunities to elucidate mechanisms of magma–crust interaction in a setting with heterogeneous S isotope signatures. We present S-isotopic data from sills and dykes on the Isle of Skye. Sharp contrasts exist between variably light $\delta^{34}S$ in Jurassic sedimentary sulphide (−35‰ to −10‰) and a local pristine magmatic $\delta^{34}S$ signature of -2.3 ± 1.5‰. Flat-lying sills have restricted $\delta^{34}S$ (−5‰ to 0‰) whereas steeply dipping dykes are more variable (−0‰ to −2‰). We suggest that the mechanism by which magma is intruded exerts a fundamental control on the degree of crustal contamination by volatile elements. Turbulent flow within narrow, steep magma conduits, discordant to sediments, and developed by brittle extension or dilation have maximum contamination potential. In contrast, sill-like conduits emplaced concordantly to sediments show little contamination by crustal S. The province is prospective for Ni–Cu–PGE mineralization analogous to the sill-hosted Noril'sk deposit, and Cu/Pd ratios of sills and dykes on Skye indicate that magmas had already reached S-saturation before reaching the present exposure level.

Supplementary material: Details of the whole-rock chemical sulphur extraction method; simplified geological maps of the Isle of Skye, a geological cross-section of part of southern Skye, and a stratigraphic log of the Mesoproterozoic and Mesozoic sediments of western Scotland; trace element diagrams of sills and dykes used in this study; and tables for QA/QC of S-isotope results, sample location information, and whole-rock major and trace element results for sill and dyke samples and for Jurassic mudrocks are available at http://www.geolsoc.org.uk/SUP18834.

Received 5 September 2014; **revised** 16 March 2015; **accepted** 19 March 2015

The Palaeogene North Atlantic Igneous Province formed from the intrusion and eruption of mantle-sourced magmas, after the impingement of the proto-Icelandic mantle plume onto overlying lithosphere. Continental rifting initiated in the Palaeogene, with an initial phase of magmatism at 62 Ma in the UK, Greenland and Baffin Island, and ultimately led to the opening of the Atlantic Ocean (continental rifting initiated *c*. 55 Ma; Saunders *et al*. 1997). The main products of this prolonged period of magmatism were tholeiitic basalts, in addition to alkali basalts. Where the mantle plume impinged on continental areas, magma fractionation, differentiation and contamination were commonplace.

The Isle of Skye and surrounding Western Isles of Scotland host a number of prominent intrusive and volcanic features of the British Palaeogene Igneous Province (Fig. 1a). On Skye, upper-crustal mafic and ultramafic intrusions were injected through Archaean Lewisian gneiss basement of the North Atlantic Craton and Mesoproterozoic Torridonian sandstones, siltstones and mudstones. At the current erosion level, the British Palaeogene Igneous Province intrusions (e.g. the flat-lying Trotternish Sill Complex and an extensive vertical suite of basalt dykes; Fig. 1a) have also penetrated through a thick succession of Mesozoic sedimentary rocks of the Hebrides Basin, which are well exposed and can be demonstrated to be physically contaminating British Palaeogene Igneous Province magmas (e.g. via the presence of xenoliths).

The sulphur content of magma may be dramatically increased during crustal contamination and may exceed the saturation concentration, triggering exsolution of an immiscible sulphide liquid into which chalcophile elements such as Cu, Ni and the platinum group elements (PGE) may partition (e.g. Naldrett 2004, 2011, and references therein). Magmas that intrude through the Jurassic mudrocks have particular potential for Ni–Cu–PGE mineralization as these sediments would be expected to contain a high level of pyrite with biogenically derived sulphur (e.g. Fisher & Hudson 1987). The source of this crustal sulphur can be established by comparing the $\delta^{34}S$ signature of the magma with that of the country rocks through which it has ascended. In crustal sediments, a substantial range of $\delta^{34}S$ compositions may be preserved in diagenetic sulphides, mostly pyrite. The sulphide isotopic range arises from mass-dependent fractionation during bacterial reduction of seawater sulphate in the contemporaneous diagenetic marine environment, which produces sulphide typically ≤20‰ lighter than the starting sulphate (Ohmoto & Goldhaber 1997). The range of $\delta^{34}S$ can range over tens of per mille (‰), with Palaeozoic and Mesozoic sulphides extending to more negative values than Precambrian rocks (Canfield & Teske 1996; Parnell *et al*. 2010). By contrast, the $\delta^{34}S$ signature of the mantle usually ranges from −2‰ to +2‰, and magmatic signatures can range from −4‰ to +4‰ depending on the oxidation state of the magma (Ohmoto & Rye 1979). Owing

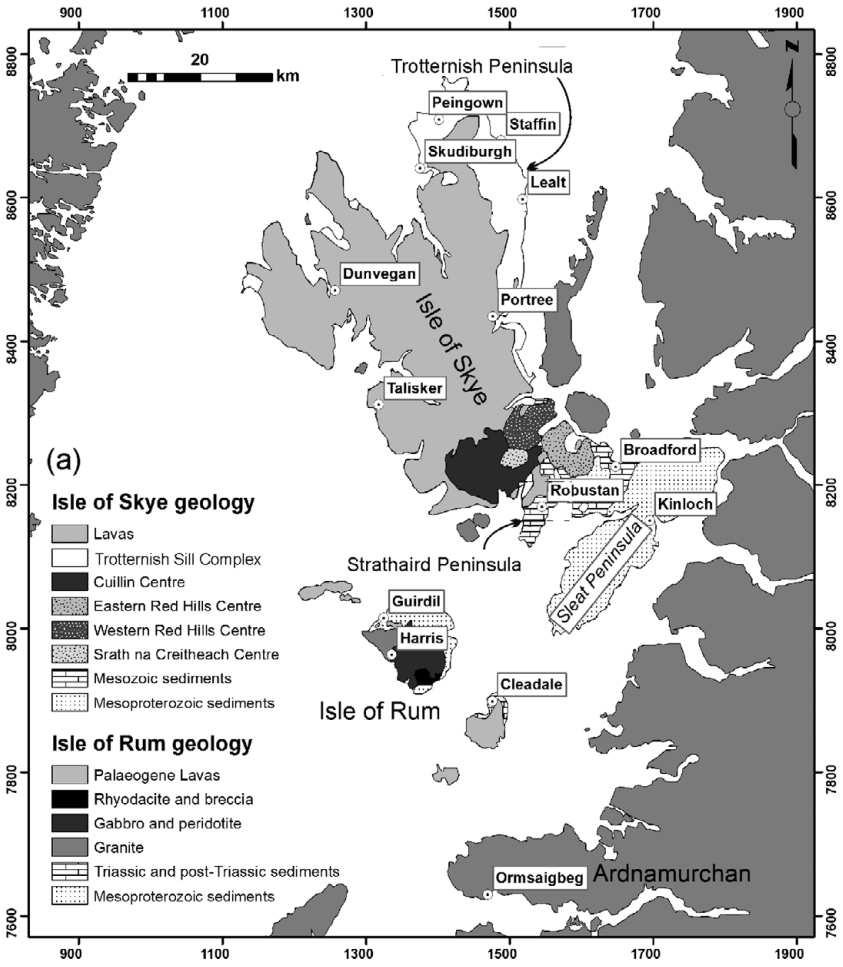

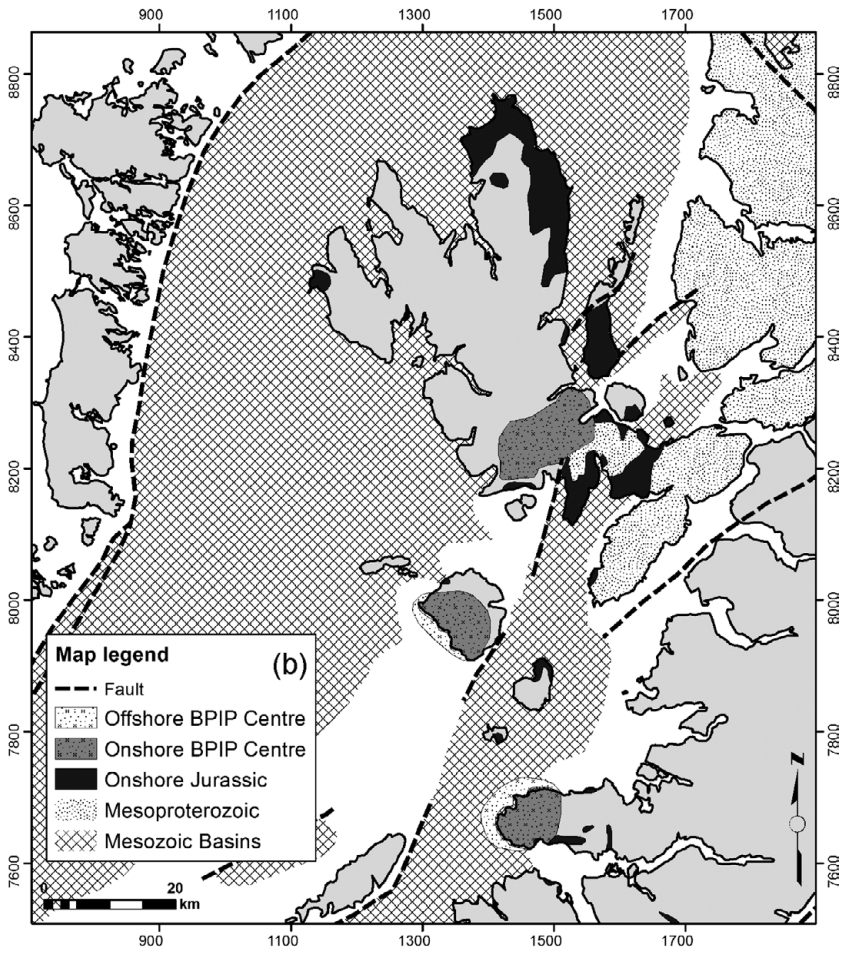

Fig. 1. (**a**) Location and simplified geological map of part of the British Palaeogene Igneous Complex (BPIP); the geology of the Isle of Skye, Rum and the Small Isles. Light grey background does not delineate specific geology, but it should be noted that the Lewisian gneisses underlie this entire region (north of the Great Glen Fault). (**b**) Hebrides Basin sediments area surrounding the Isle of Skye and the Small Isles. Adapted from Fyfe *et al.* (1993).

to the dynamic nature of magma intrusion, the crustal S-isotopic signature may be transported away from the immediate site of contamination throughout magma ascent. Therefore crustal S input could be detected remotely from concentrated sulphide mineralization. Such contamination is typically revealed by analysis of S isotopes in sulphide minerals or whole-rock samples. Our study uses and develops both techniques to test for crustal contamination in the British Palaeogene Igneous Province. The addition of crustal sulphur to a magmatic system is commonly considered essential in the formation of orthomagmatic Ni–Cu–PGE mineralization (e.g. Naldrett 2004, 2011; Ripley & Li 2013) and hence identifying the controls on crustal sulphur contamination, and where this may be occurring, will refine strategies for targeting of Ni–Cu–PGE orthomagmatic mineralization in the British Palaeogene Igneous Province and elsewhere.

We present the first published sulphur isotope compositions for the British Palaeogene Igneous Province, determining a 'framework' for the country rock $\delta^{34}S$ of the Hebrides Basin compared with $\delta^{34}S$ of the British Palaeogene Igneous Province upper-crustal intrusions on Skye (including samples from the Lewisian basement, Torridonian sediments, and various Jurassic sediments of the Hebrides Basin). We identify the 'background' plume magmatic sulphur isotopic composition of the British Palaeogene Igneous Province, and investigate if widespread crustal sulphur contamination of magmas took place in NW Scotland. Coupled with whole-rock Ni, Cu and PGE concentrations, this contributes towards the development of a new model for magmatic sulphur contamination, dependent on the mechanism (orientation and energy) by which magma is intruded through a conduit, which affects near-field exploration models for orthomagmatic Ni–Cu–PGE deposits.

Geology of the Hebridean portion of the British Palaeogene Igneous Province

The British Palaeogene Igneous Province is part of the earliest magmatic series of the North Atlantic Igneous Province, which includes Palaeogene rocks of the Hebridean Igneous Province (along the west coast of Scotland) and Northern Ireland (Fig. 1a). In Scotland, the British Palaeogene Igneous Province includes the Isles of Mull, Skye, Arran, the Small Isles (Rum, Eigg, Muck, Canna and Sanday), together with the mainland igneous complex of Ardnamurchan and lava flows of Morvern. Thus, the British Palaeogene Igneous Province in Scotland extends over a number of tectonic terranes.

Crustal impingement of mantle-sourced mafic magmas resulted in subaerial eruptions along fissure-type feeders (Kent *et al*. 1998), now seen as a laterally continuous linear array of dyke swarms, with single dykes typically <10 m wide (Emeleus & Bell 2005). These NW–SE-trending dykes are perpendicular to the North Atlantic rift margin and indicative of the contemporaneous NE–SW-directed extension of NW Europe at this time (Emeleus & Bell 2005). Sills associated with lava fields and central complexes normally occur within Mesozoic sediments below lavas, suggesting a relatively shallow emplacement depth (probably <1 km). Single sill thicknesses are up to tens of metres, amalgamating to form complexes hundreds of metres in thickness. Sills are often observed to have their own compositional characteristics, unrelated to other overlying lavas. Sills predominantly consist of alkali olivine basalts and tholeiitic basalts, although trachytes and rhyolites are recognized as minor fractionation products (Emeleus & Bell 2005).

Palaeogene geology of the Isle of Skye

The Isle of Skye records numerous exposures of British Palaeogene Igneous Province magmatic rocks injecting through and into a thick Mesozoic sedimentary sequence, part of the Hebrides Basin (Harker 1904). Below the Mesozoic rocks, a thick crustal pile of deformed Neoproterozoic (Torridon and Sleat Group) sediments are present above Archaean (Lewisian) basement (Fig. 1b). Hence the Isle of Skye provides an excellent opportunity to study the sources, extent and controls on crustal sulphur contamination in a continental rift environment.

The Trotternish Sill Complex, northern Skye

The Trotternish Sill Complex crops out on the Trotternish Peninsula on the north of the Isle of Skye intruding Jurassic sandstones, limestones and marls (Fig. 1a; Gibb & Gibson 1989). The picrites, picrodolerites, and crinanites (analcite olivine dolerites) present throughout the sill complex are genetically related, and thought to result from differentiation of an alkali–olivine basalt magma (Gibson & Jones 1991) with varying crustal contamination (Simkin 1967; Gibson 1990). This horizontal sill complex post-dates the Skye Lava Group and is at least 250 m thick, with single sills measuring tens of metres in thickness. Rafts or 'packages' of Jurassic sediments (now baked) occur sporadically within the thickness of the Trotternish Sill Complex in various locations. Sills can display multiple and composite lithologies or melt generations, with banding commonplace (Gibson & Jones 1991; Emeleus & Bell 2005). In these cases, the lower zones of a sill are the most mafic. For a detailed 'stratigraphy' of the Trotternish Sill Complex, the reader is referred to Gibson (1990) and Gibson & Jones (1991).

Dykes from the Robustan area of the Strathaird Peninsula, southern Skye

Dyke swarms on the Isle of Skye are predominantly directed in a NW–SE azimuth and caused significant local crustal dilation. Most dykes are <1 m thick, but some wider dykes (e.g. Strathaird Peninsula) display evidence of incremental build-up owing to multiple mafic magma injections, resulting in magma mingling and layering within dykes (Platten 2000). The Skye Dyke Swarm intrudes both lavas and gabbros of the Cuillin Centre, and the dykes are cut by cone-sheets (Bell & Williamson 2002). Compositionally, the Skye Dyke Swarm ranges from silicic pitchstones, to alkali and tholeiitic basalts, and trachytes (Emeleus & Bell 2005). Ultramafic dykes are predominantly found closest to the Cuillin Central Complex.

At Robustan on the Strathaird Peninsula, southern Isle of Skye (see Fig. 1a), abundant NNW–SSE- to NW–SE-trending basaltic dykes (hereafter called 'Robustan dykes') cross-cut both the lavas and sediments (see cross-section, Fig. 2). They represent part of a larger dyke swarm, formed and intruded after the eruption of the Strathaird lavas, and after the intrusion of the Cuillin Central Complexes to the north and NW. The cross-section in Figure 2 displays the transect from which dyke and sediment samples were collected. Rare or minor examples of more evolved dyke compositions are also observed, including basaltic trachyandesites. The dykes are typically vertical and range from 30 cm to 10 m in width. The dykes are finely crystalline (crystal size <1 mm) and equigranular. Chilled margins are usually absent.

Stratigraphy of the Hebrides Basin and potential for crustal S contamination

The Mesoproterozoic Torridonian succession of NW Scotland (Fig. 1b) divides into the Sleat, Stoer and Torridon Groups. It is dominated by sandstones and psammites (Stewart 2002; Kinnaird *et al*. 2007). Minor siltstone and mudrock units are thinner and less extensive than in the overlying Jurassic units. Recent sulphur isotope studies of Torridonian sulphates and sulphides from the far NW of Scotland (Stoer to Gruinard Bay) have identified an isotopic shift in $\delta^{34}S$ associated with bacterial

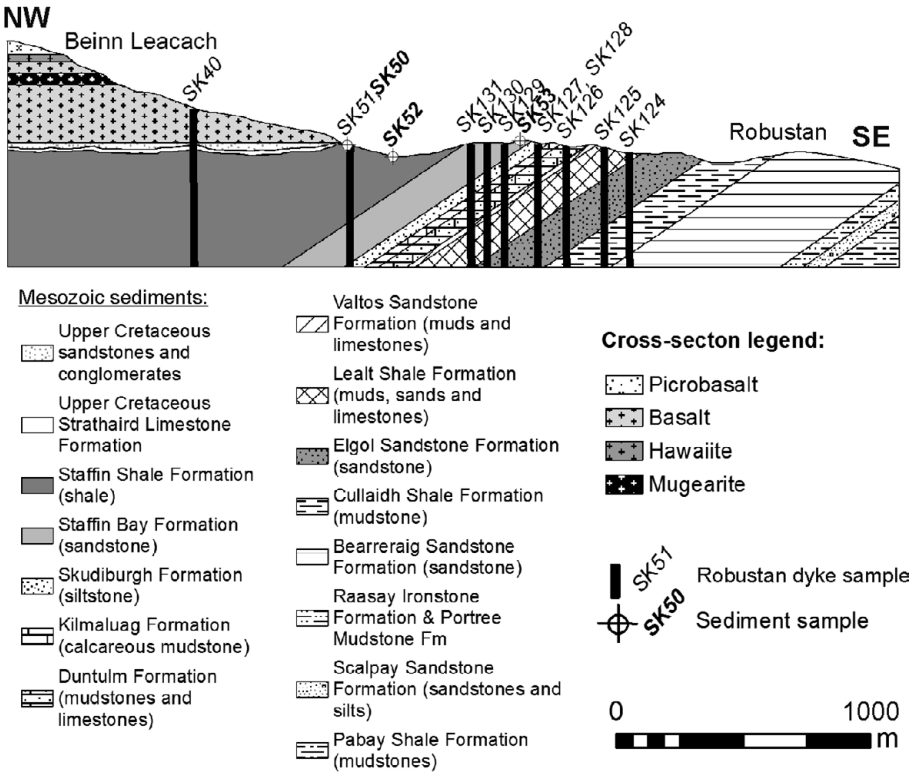

Fig. 2. Strathaird Peninsula (southern Skye). Line of cross-section displays position of the dyke samples as projected parallel to the strike of the sediment bedding planes, with the exception of sample SK40, which has been projected onto the cross-section along the strike of the dyke itself. Dykes drawn assuming vertical dip. Sediments dip *c*. 10° NNW below the sediment–lava contact at Scaladal Burn (note cross-section shows 2× vertical exaggeration). Extent of dyke structure under the current surface level is unknown; cross-section projects dykes for display purposes only.

sulphate reduction, highlighting that the Mesoproterozoic terrestrial environment was adequately oxygenated to support life (Parnell *et al*. 2010, 2012). For example, pyrite-bearing lacustrine siltstones of the Diabaig Formation (basal Torridonian) have $\delta^{34}S$ compositions of −30.1 ± 17.3‰. During the present study, 14 Torridonian, Sleat, and Stoer Group sediment samples were collected from the Isle of Skye and Rum for sulphur isotopic analysis. Of these, only five samples yielded enough sulphide precipitate (following whole-rock sulphur extraction; see 'Methods' section below) to allow for conventional S-isotope analysis.

The anticipated sulphur concentration of the Lewisian crystalline basement and Mesoproterozoic sediments is significantly lower than in the Mesozoic Hebrides Basin, so although the S-isotopic composition of all of these potential contaminants was analysed during this study, the main focus is laid on the Mesozoic. The sedimentary stratigraphy of the Mesozoic Hebrides Basin is presented in Figure 1b (based on Morton & Hudson 1995; Hesselbo & Coe 2000). Although several literature sources have documented the carbon and oxygen isotopic composition of these rocks, only Yallup *et al*. (2013) reported the sulphur isotopic composition of a single unit (in the Middle Jurassic Cullaidh Shale Formation; mean bulk-rock $\delta^{34}S$ –0.7 ± 1.8‰). Sulphur isotopes for Jurassic sediments from elsewhere in the British Isles have been reported (e.g. Raiswell *et al*. 1993; Hudson *et al*. 2001); however, until now there has been no Hebridean 'stratigraphy' of sulphur isotopes available to establish an S-isotope framework of potential contaminants to British Palaeogene Igneous Province magmas. In the present study, the Palaeogene igneous rocks of interest are observed intruding through, and physically being contaminated by Jurassic sedimentary sequences (via the presence of xenoliths). Thus, it is specifically the Jurassic units that are of most interest for the purposes of this study. This is due to the high proportion and volume of S-rich shales and mudrocks throughout this Jurassic succession, unlike in the older Triassic or younger Cretaceous sediments that are sulphur poor and sporadically developed across the region (e.g. Hesselbo & Coe 2000).

The Trotternish Sills intrude through the same thick package of Jurassic sediments as the Robustan dykes on the Strathaird Peninsula. Thus equivalent Jurassic sedimentary rocks are present as potential contaminants to ascending British Palaeogene Igneous Province magmas and allow for the two different types of intrusive body (sill v. dyke) to be tested against one another for their degree of crustal S contamination.

Methods

Sampling strategy

In northern Skye, 23 Trotternish Sill Complex samples were collected, including a range of all rock types (picrites, picrodolerites and crinanites). Of these, 11 samples were analysed for sulphur isotopes, and PGE and Au.

At Lealt Quarry [NG 5188 6064], a finely crystalline dyke (crystals <0.5 mm) *c*. 2 m wide (strike 338°) with a vertical orientation cuts the Trotternish Sill Complex (comprising an upper crinanite sill, overlying a picrite sill and pegmatitic picrite sill; Fig. 3a). The dyke contains 2–20 cm elongate xenoliths of a baked mudrock (probably of Jurassic origin) and 5–10 cm picrite sill xenoliths at its margins (Fig. 3b). The dyke appears to be compound with faint vertical banding (showing indistinct boundaries) at its centre, and elongate xenolith trails within some bands (Fig. 3c). This indicates multiple injections of basalt in the dilatational fracture through which the dyke has intruded. Disseminated millimetre-scale (2–10 mm) pyrite crystals are associated with these xenoliths and occur at the dyke margins, with most disseminated pyrite mineralization at the contacts with mudrock xenoliths, or forming 'stringers' through the basalt dyke within 30 cm of the xenoliths. There are also trails of white-coloured zeolites (2–10 mm diameter) within 20 cm of the dyke margin (Fig. 3d). Four samples from the Lealt Quarry basaltic dyke, which cross-cuts the sill units and four Jurassic sediment samples from packages adjacent to or within the Trotternish Sill Complex, were also collected from northern Skye (e.g. Fig. 3e).

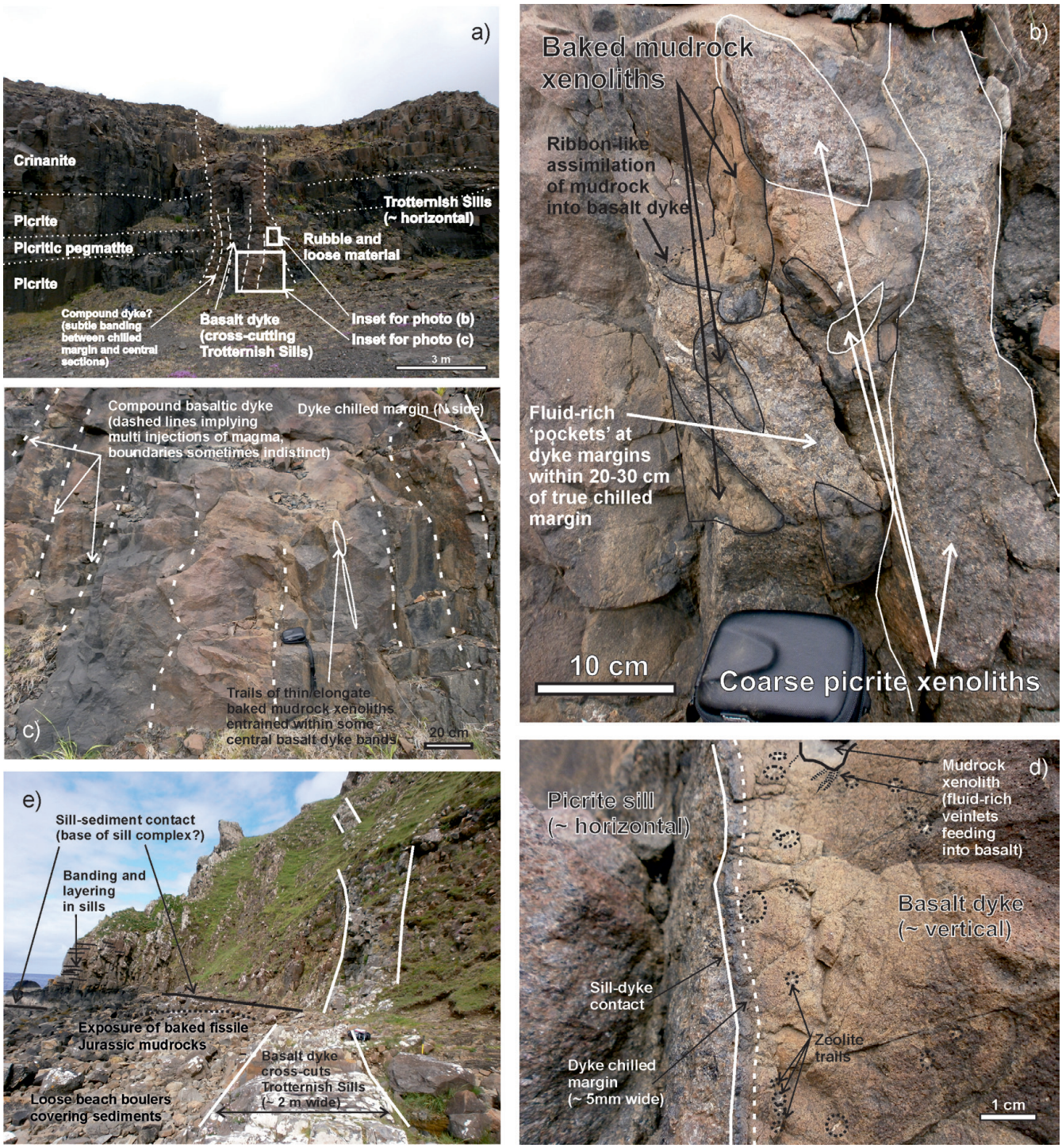

Fig. 3. Annotated photographs of field relations for the Trotternish Sills and cross-cutting dykes on the Trotternish Peninsula. (**a**) Lealt Quarry (looking west); horizontal Trotternish Sills cross-cut by a later, banded basalt dyke. (**b**) Close-up of northern margin of basalt dyke in Lealt Quarry showing both picrite (white lines) and mudrock (black lines) xenoliths in a fluid-rich coarser section of the dyke *c*. 10 cm from the chilled margin. Some mudrock xenoliths have begun to disintegrate and 'fray' at the edges, becoming assimilated or with ribbon-like fluid-rich trails extending into the basalt. (**c**) Faint banding in the central portions of the dyke. Some 'bands' have elongate mudrock xenolith trails. (**d**) Close-up of the southern margin of the basalt dyke at Lealt Quarry showing trails of white zeolites close to the chilled margin (outlined by black dashed circles). Baked mudrock xenolith with white-coloured fluid-rich stringers extending into basalt is shown at top of the image. Basalt dyke contact with picrite sill is indicat by continuous white line, and *c*. 5 mm wide basalt chilled margin by dashed white line. (**e**) Skudiburgh, looking north, with vertical basalt dyke cross-cutting the horizontally banded Trotternish Sills. There are no offsets of dyke or sills, despite the angle of the photograph. Black continuous line indicates base of the sill package, which overlies a poorly exposed area of baked mudrocks (best observed in the area indicated by dashed black line).

In southern Skye, one basaltic trachyandesite and eight basaltic dyke samples were collected from a NW–SE-oriented transect *c*. 1 km in length through the Jurassic succession at Robustan (Fig. 2). All dykes ranged between 30 cm and 8 m in width, with most measuring 1–2.5 m wide. One dyke (SK51) displayed rare quartz-filled amygdales up to 0.5 cm in diameter; however, all other sampled dykes were amygdale-free. Dyke samples SK124 and SK129 contained visible pyrite within 5 cm of the dyke contact with sediments. Samples were collected from a mixture of dyke margins and central zones. In southern Skye, five samples of the Jurassic

sediments were collected from this area, including shales, a siltstone and sandstones.

Whole-rock geochemistry

Major and trace element analyses (including PGE and Au) and S-isotopic ($\delta^{34}S$) results are given in Table 1. A selection of igneous and sedimentary samples were also analysed for elemental S abundance. Sediment S-isotopic compositions and S concentrations, spanning the upper portion of the Lower to the Upper Jurassic, are presented in Table 1, and a sub-selection of four sediments were analysed for their major and trace element geochemistry. For the Lower Jurassic, samples were obtained from outcrops on the Ardnamurchan Peninsula, mainland Scotland. In addition, we analysed the S-isotopic composition of two sulphide-bearing samples from the Lewisian gneisses of NW Scotland (X66 and X11b), and one sample of Moine metapelite from Ardnamurchan (AN78; Table 1).

Unweathered material was crushed, split and milled to a fine powder in an agate planetary ball mill. Major and trace elements were analysed by inductively coupled plasma optical emission spectrometry (ICP-OES; JY Horiba Ultima-2) and inductively coupled plasma mass spectrometry (ICP-MS; Thermo X Series 2) respectively at Cardiff University using methods and instrumentation described by McDonald & Viljoen (2006). PGE and Au analysis for samples was carried out by Ni-sulphide fire assay followed by Te co-precipitation and ICP-MS (Huber *et al*. 2000; McDonald & Viljoen 2006). Accuracy for whole-rock elemental geochemistry was constrained by analysis of the certified reference materials TDB1 and WMG1 for PGE and Au, and JB1a for all other trace and major elements. Precision was determined by repeat analysis of a subset of samples, with most elements repeatable to within 10% or better.

Sulphur isotope analyses

Samples with visible sulphide minerals >500 μm^2 were cut into blocks (up to 40 × 20 mm in area) and polished. *In situ* laser combustion of polished sulphides was carried out following the technique of Wagner *et al*. (2002). Based on experimental results, laser combustion causes a small and predictable fractionation of sulphur isotope compositions for $\delta^{34}S$ of the SO_2 gas produced, compared with the actual $\delta^{34}S$ of the sulphide mineral (Wagner *et al*. 2002). Therefore the raw $\delta^{34}S$ data were corrected by the following factor: $\delta^{34}S_{pyrite} = \delta^{34}S_{SO2laser} + 0.8‰$. Whole-rock S extracted from the rocks (see below), and a series of samples from which sulphide separates could be picked, were analysed following the technique of Robinson & Kusakabe (1975).

SO_2 gas samples were analysed at the Scottish Universities Environment Research Centre (SUERC) using a ThermoFisher Scientific MAT 253 dual inlet mass spectrometer (for conventional samples) and an on-line VG Isotech SIRA II mass spectrometer (for laser combustion samples). Standards used throughout all analyses were IAEA-S-3 and NBS-123 international standards, alongside an SUERC laboratory chalcopyrite standard, CP-1. The results for these gave −31.5‰ (IAEA-S-3, certified to be −31.5‰), −4.5‰ (CP-1, certified −4.6‰) and +17.1‰ (NBS-123; certified +17.1‰), with $2\sigma < \pm 0.2‰$ reproducibility, based on repeated standard analyses. All data are reported in standard per-mille variations from the Vienna Cañon Diablo troilite standard, V-CDT.

Our Chromium Reducible Sulphur (CRS) sulphide extraction procedure (for whole-rock powders) is based on and adapted from numerous published and unpublished procedures (Zhabina & Volkov 1978; Canfield *et al*. 1986; Tuttle *et al*. 1986; Hall *et al*. 1988; Newton *et al*. 1995; Nielsen & Hanken 2002; Labidi *et al*. 2012).

Whole-rock sulphur concentration analysis

A selection of powdered rock samples were analysed for bulk-rock S concentration by LECO CS230 Carbon/Sulphur Determinator at the University of Leicester, UK. Between 0.1 and 1.0 g of sample was used depending on relative bulk S content. Samples were ignited in an O_2 stream and the SO_2 produced was analysed by IR absorption. Each sample was run in triplicate to monitor precision. Accuracy was monitored by regular analysis of the reference material BAS ECRM 877-1. The limit of minimum detection for this method is 0.018 wt% S, which is calculated based on 3 × standard deviation of the mean blank value. A total of 11 samples (both British Palaeogene Igneous Province intrusive rocks and sedimentary rocks) were analysed by this method.

Results of $\delta^{34}S$ and S determinations

Trotternish Sill Complex

The $\delta^{34}S$ of the Trotternish Sill Complex (including samples from the chilled margins at the base of the sill complex) ranges from +0.1‰ to −4.9‰; however, sample SK102 from 2 m above the base of the complex at Skudiburgh gave −10.8‰ (Fig. 4). Excluding sample SK102, the mean $\delta^{34}S$ of the Trotternish Sills is $-2.3 \pm 1.5‰$. Total PGE concentrations for these sills range from 12.6 to 30.9 ppb with no clear correlation between whole-rock total PGE content and whole-rock $\delta^{34}S$. Whole-rock Pd concentration ranges from 2.1 to 10.2 ppb and Cu from 57 to 252 ppm (Fig. 5). The Cu/Pd ratio varies from 13300 to 46200 with two anomalously high ratios of 72800 and 81100 (samples SK89 and SK83, respectively; SK83 is from the base of the picrite sill complex at Dunflodigarry, $\delta^{34}S = -4.9‰$). Pd/Ir ratio ranges from 3.1 to 14.1 with an anomalous value of 56.5 for sample SK90 (a pegmatitic picrite sill from Lealt Quarry, $\delta^{34}S = -2.2‰$). Overall, Pt/Pd ratio for the sills varies from 0.94 to 2.55.

The basaltic dyke at Lealt Quarry, which cross-cuts the Trotternish Sill Complex (Fig. 3a and b), has a $\delta^{34}S$ of −7.5‰ at the margins (Fig. 4a), where the dyke has entrained baked mudrock xenoliths ($\delta^{34}S$ signature of −15.4‰; Fig. 6). At the centre of the dyke, where xenoliths are absent, the basalt has $\delta^{34}S = -6.5‰$. At the dyke margin, the total whole-rock PGE concentration is 17.9 ppb, as opposed to 1.18 ppb at the dyke centre. Cu/Pd ratio at the margin is 18650 but is significantly higher in the centre of the dyke (77800). Pt/Pd and Pd/Ir show little variance from the dyke margin to its centre, ranging from 12.1 to 14.1 and from 1.02 to 1.35 respectively.

Robustan dyke swarm

The $\delta^{34}S$ of eight samples of basaltic dykes from Robustan ranges from −2.3‰ to −30.7‰ (Table 1, Fig. 4a). Sample SK131 (from the centre of a 30 cm wide basalt dyke) gave the lightest $\delta^{34}S$, at −30.7‰, and has a measured whole-rock sulphur concentration of 1.339 wt%. Sample SK129 (from the centre of an 80 cm wide basalt dyke) gave 0.408 wt% S and −15.5‰, and SK127 (from the centre of a 2.5 m wide dyke) has 0.122 wt% S and −5.1‰. This distribution of S-isotope composition and S concentration indicates a strong correlation between the S-isotope signature and concentration of S in the dykes (Fig. 4b), dykes with a higher concentration of S having significantly lower $\delta^{34}S$ (correlation $r^2 = 0.98$). A basaltic trachyandesite, SK130, with *c*. 1 mm diameter rounded pyrite crystallized in some portions of the dyke (mostly at the margins) produced $\delta^{34}S$ of $-19.8 \pm 1.4‰$.

Total whole-rock PGE concentrations in the dykes range from 6.4 to 52.4 ppb, and Pd ranges from 1.25 to 16.2 ppb (Fig. 5a). Cu concentration ranges from 90.3 to 207 ppm (Fig. 5b). Cu/Pd ratios vary between 5590 and 167200. Pd/Ir varies from 11.9 to 48.8 and

Table 1. *Summary of sulphur isotopic compositions ($\delta^{34}S$) measured by conventional method (following whole-rock sulphur extraction; indicated as 'wr') and laser combustion method (indicated as 'laser')*

Sample number				Analytical method	$\delta^{34}S$ (‰)	S (wt%)
Sedimentary	Period	Group, Formation, Member	Sediment type			
SK50	Upper Jurassic	Staffin Shale Formation	Shale	Laser	−32.6	0.113
SK52	Upper Jurassic	Staffin Shale Formation	Siltstone	wr	−29.2	–
SK53	Upper Jurassic	Staffin Bay Formation	Sandstone	wr	−33.8	<0.02
SK103	Middle Jurassic	Skudiburgh Formation, Great Estuarine Group	Fissile, baked mudrock	wr	No precipitate	–
SK108	Middle Jurassic	Kilmaluag Formation, Great Estuarine Group	Marl	wr	No precipitate	–
SK93b	Middle Jurassic	Unknown, probably Great Estuarine Group, Lealt Shale Formation	Baked mudstone xenolith	Laser	−15.4	–
AN69	Lower Jurassic	Lias Group, Raasay Ironstone Formation	Ironstone	wr	−14.7	–
AN71	Lower Jurassic	Lias Group, Raasay Ironstone Formation	Pyrite nodule in ironstone	Laser	−18.4	27.7*
AN68	Lower Jurassic	Lias Group, Portree Shale Formation	Recrystallized mudstone	wr	−17.6	–
RM78	Mesoproterozoic	Torridon Group, Aultbea Formation	Sandstone	wr	No precipitate	–
RM3	Mesoproterozoic	Torridon Group, Applecross Formation	Sandstone	wr	+1.4	–
RM5	Mesoproterozoic	Torridon Group, Applecross Formation	Sandstone	wr	+3.0	–
RM82	Mesoproterozoic	Torridon Group, Diabaig Shale Formation	Shale	wr	No precipitate	–
SK118	Mesoproterozoic	Sleat Group, Kinloch Formation	Mudstone	wr	+4.7	<0.02
SK114	Mesoproterozoic	Sleat Group, Beinn na Seamraig Formation	Sandstone	wr	+2.6	–
SK117	Mesoproterozoic	Sleat Group, Loch na Dal Formation	Grit	wr	+2.0	–
AN78	Neoproterozoic	Moine coarse micaceous metapelite	n/a	wr	+2.5	–
Basement	Period	Lithology				
X66	Archaean	Lewisian amphibolite pod (with minor pyrite), Assynt Terrane		wr	+1.2	–
X11b	Archaean	Lewisian ultrabasic amphibolite (with minor pyrite), Assynt Terrane		wr	−1.4	–
Igneous	Location	Description	Feature type			
SK83	Dunflodigarry	Picrite sill (sampled from base of cliff on beach)	Picrite sill	wr	−4.9	<0.02
SK89	Staffin	Crinanite sill sampled 20 m above contact with limestones	Crinanite sill	wr	–	–
SK90	Lealt Quarry	Pegmatite band in picrite sill	Pegmatitic picrite	wr	−2.2	0.0326
SK92	Lealt Quarry	Picrite sill *c*. 2 m below pegmatite band	Picrite sill	wr	−1.7	–
SK93a	Lealt Quarry	East margin of basalt dyke with baked mudrock xenolith bearing pyrite, dyke *c*. 2 m wide	Basalt dyke	wr	−7.5	–
SK96	Lealt Quarry	Basalt dyke (centre), dyke *c*. 2 m wide	Basalt dyke	wr	−6.5	–
SK100	Skudiburgh	Chilled picrite at base of sill complex	Picrite sill	wr	−2.6	<0.02
SK101	Skudiburgh	Finely crystalline picrite (crystals <0.5 mm), located *c*. 50 cm above base of sill complex	Picrite sill	wr	−3.1	–
SK102	Skudiburgh	Medium crystalline picrite (crystals <1 mm), located *c*. 2 m above base of sill complex	Picrite sill	wr	−10.8	<0.02
SK104	Skudiburgh	Picrite sill sampled *c*. 30 m above base of sill	Picrite sill	wr	–	–
SK109	Peingown	Base of picrodolerite sill (sampled from chilled margin at contact)	Picrodolerite sill	wr	−2.3	–
SK110	Peingown	Picrodolerite sample located *c*. 50 cm above base of sill	Picrodolerite sill	wr	+0.1	–
SK124	Robustan	Basalt dyke (margin), dyke *c*. 1 m wide	Basalt dyke	wr	−3.7	–
SK125	Robustan	Basalt dyke (margin), dyke *c*. 1 m wide	Basalt dyke	wr	−2.3	–
SK126	Robustan	Basalt dyke (centre), dyke *c*. 1 m wide	Basalt dyke	wr	−2.9	–
SK127	Robustan	Basalt dyke (centre), dyke *c*. 2.5 m wide	Basalt dyke	wr & laser	−5.1	0.122
SK128	Robustan	Basalt dyke (centre), dyke *c*. 2.0 m wide	Basalt dyke	wr	−3.9	–
SK129	Robustan	Basalt dyke (centre), dyke *c*. 80 cm wide	Basalt dyke	wr & laser	−15.5	0.408
SK130	Robustan	Basaltic trachyandesite dyke (margin), dyke *c*. 1.5 m wide	Basaltic trachyandesite dyke	wr & laser	−19.8	–
SK131	Robustan	Basalt dyke (centre), dyke *c*. 30 cm wide	Basalt dyke	wr	−30.7	1.34
SK51	Robustan	Basalt dyke (centre), dyke at least 6 m wide (contacts not clearly visible)	Basalt dyke	wr	−14.1	–

Whole-rock S concentration (in wt%) is also listed. 'No precipitate' indicates that a powdered sample was subjected to the whole-rock sulphur extraction (CRS) method but no precipitate was yielded or the precipitate was too small to facilitate conventional analysis. Samples with S concentration below detection limit are indicated by <0.02 (detection limit). n/a, not applicable.

*The S concentration of this sample was too high to be determined (based on the calibrated set-up of LECO) and thus the estimated S concentration is listed.

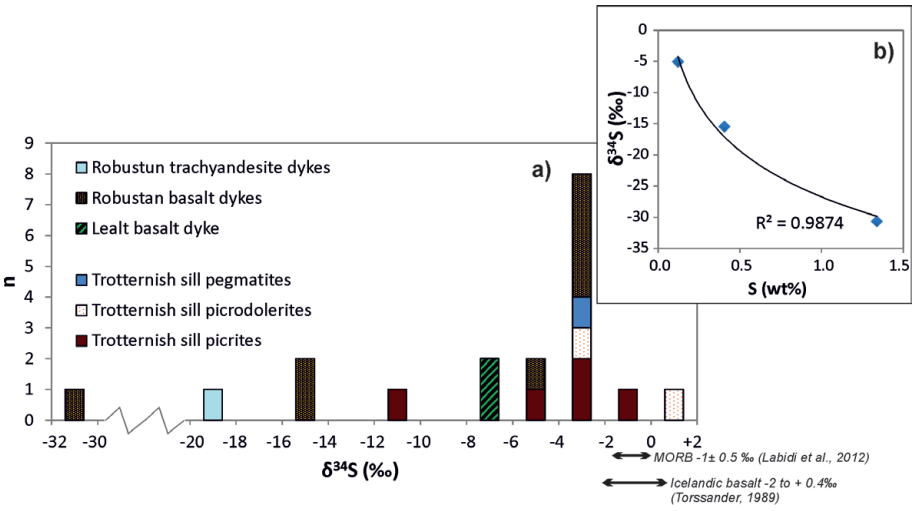

Fig. 4. Sulphur isotope ($\delta^{34}S$) results for Isle of Skye sills and dykes. (**a**) All sills and dykes. (**b**) Correlation between whole-rock S concentration and $\delta^{34}S$ for Robustan dykes (line of best fit is a logarithmic fit as shown, but a linear fit also produces r^2 value >0.95).

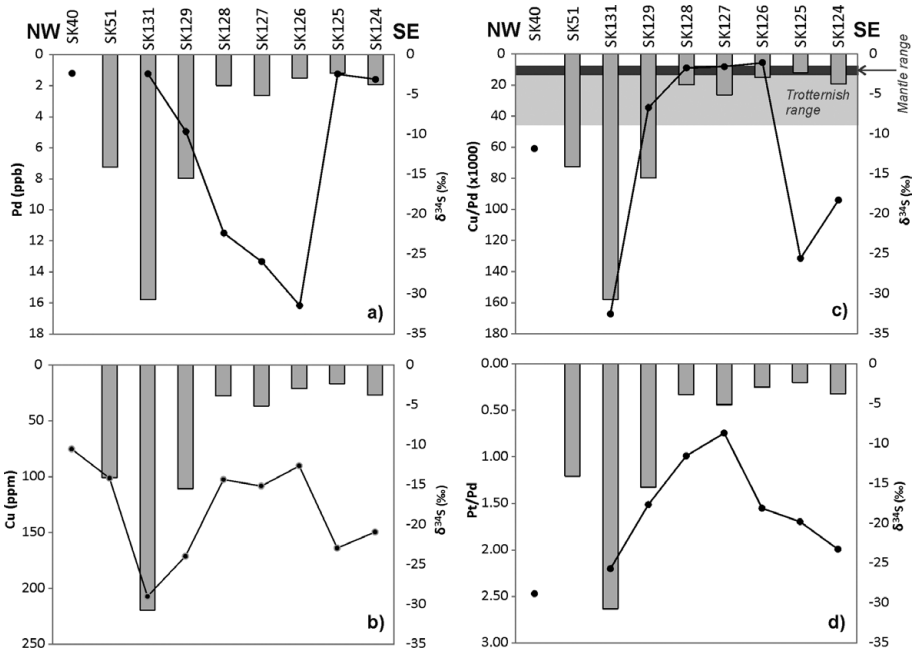

Fig. 5. Sulphur isotope ($\delta^{34}S$) results (grey histograms) and whole-rock PGE and Cu concentrations and ratios (black lines with circles) for the basaltic Robustan dykes, aligned according to a NW–SE transect, as displayed in the cross-section of Figure 2. (**a**) Pd (ppb) and $\delta^{34}S$; (**b**) Cu (ppm) and $\delta^{34}S$; (**c**) (Cu/Pd) × 1000 ratio and $\delta^{34}S$; (**d**) Pt/Pd ratio and $\delta^{34}S$. The light grey band in (**c**) indicates the range of Cu/Pd ratios measured in samples from the Trotternish Sill Complex and dark grey band indicates mantle ranges (according to McDonough & Sun 1995).

Pt/Pd ratio ranges from 0.74 to 2.20. The Cu/Pd and Pt/Pd ratios of the dykes are chiefly controlled by Pd concentration (Fig. 5c and d). Transposing all samples onto a NW–SE-oriented section (Figs 2 and 5) we observe that the $\delta^{34}S$ composition of the dykes becomes significantly lighter from SE to NW. This broadly coincides with an increase in the stratigraphic level of the Jurassic sediments that the dykes cross-cut, and into which they intrude. Arranging the results in this manner, we see that between samples SK126 and SK131 a sharp decrease in Pd concentration coincides with a considerable shift in $\delta^{34}S$ (from −2.9‰ to −30.7‰ respectively) and a sharp rise in Cu/Pd (Fig. 5c). Pt/Pd broadly follows this increasing Cu/Pd trend from SE to NW (Fig. 5d); however, SK126 is anomalous owing to the significantly higher Pt concentration (25.1 ppb) in this sample.

Sedimentary and contaminant country rock units

Of the Jurassic sediments collected from Robustan (Fig. 2) and analysed by whole-rock sulphur extraction and conventional analysis, the shale member of the Staffin Shale Formation and the Staffin Bay Formation Carn Mor Sandstone Member have the lightest sulphur isotopic signature, with $\delta^{34}S = -32.6$‰ and −33.8‰ respectively (Table 1, Fig. 6). The measured sulphur concentration of the shale was 1130 ppm S, but the concentration of sulphur in the sandstone was below detection limit (<180 ppm). A siltstone member of the Staffin Shale Formation also yielded an average $\delta^{34}S = -29.2$‰. As mentioned above, the assumed Jurassic mudrock xenolith in the Lealt Quarry basalt dyke produced $\delta^{34}S = -15.4$‰. Samples of the Staffin Shale Formation (SK103) and Kilmaluag Formation marl (SK108) have very low concentrations of sulphur. Similarly low or absent S contents were recorded in Duntulm Formation limestone. A recrystallized mudstone (Portree Shale Formation) and two ironstone samples (Raasay Ironstone Formation with abundant pyrite nodules) from Ardnamurchan produced $\delta^{34}S = -17.6$‰ and −14.7‰ respectively. The pyrite-rich nodules themselves had $\delta^{34}S = -18.4$‰ but had the highest concentration of S with up to 28 wt% (Table 1).

The two pyrite-bearing samples of Lewisian amphibolite gneiss collected from the Assynt Terrane in NW Scotland gave a $\delta^{34}S$ of −1.4‰ to +1.2‰. The Moine metapelite from the Ardnamurchan Peninsula produced $\delta^{34}S = +2.5$‰. Torridon and Sleat Mesoproterozoic sediments collected from the Isles of Skye and Rum (Fig. 6a) have $\delta^{34}S$ ranging from +1.4‰ to +4.7‰, although few samples out of the total number collected had sufficient S to produce a usable whole-rock Ag_2S precipitate. Samples

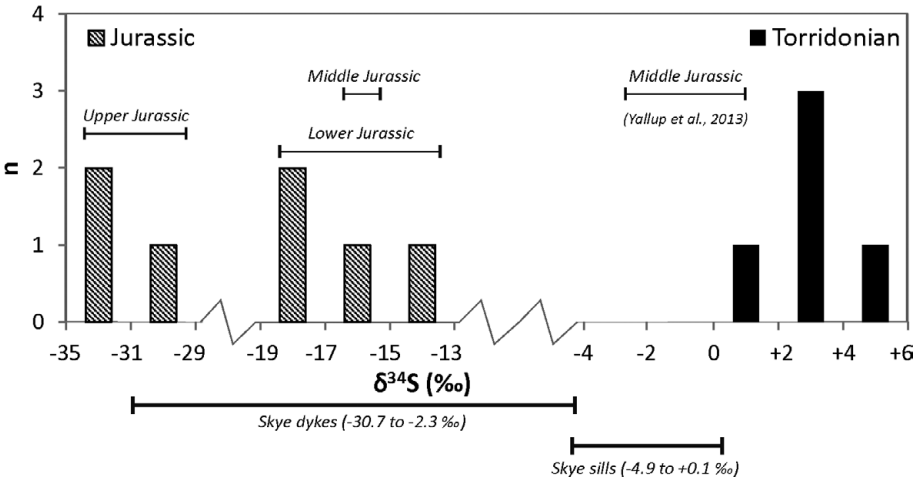

Fig. 6. Sulphur isotope ($\delta^{34}S$) results for Jurassic and Torridonian (Mesoproterozoic) sediment samples from the Hebrides Basin area, Isle of Skye, Isle of Rum and Ardnamurchan.

from the Aultbea Formation sandstone and a shale from the Diabaig Formation were S poor and did not yield sufficient precipitate for analysis. Together with the Archaean Lewisian gneisses and Moine metasediments, the Mesoproterozoic lithologies delineate a limited range of $\delta^{34}S$, from −1.4‰ to +4.7‰, with a mean of +2.0 ± 1.8‰. This is clearly distinct from the mean Jurassic sediment $\delta^{34}S$ of −21.5 ± 8.0‰ (e.g. Fig. 6) and offers the potential to act as a tracer of upper shallow crustal contamination in the British Palaeogene Igneous Province intrusive suites.

Discussion

The results of this study provide the first comprehensive S-isotope framework for the British Palaeogene Igneous Province through determining the regional crustal signatures and those of the British Palaeogene Igneous Province magmas on Skye. Our work has identified the following key features.

(1) Local Precambrian basement has a limited range of $\delta^{34}S$ values (−1.4‰ to +4.7‰) with a mean of +2.0 ± 1.6‰, which overlaps typical magmatic values. This contrasts markedly with the Mesoproterozoic values found on the mainland by Parnell *et al*. (2010).

(2) Local Jurassic sediments have a distinct light $\delta^{34}S$ signature ranging −35‰ to −10‰ and a mean of −21.5 ± 8.0‰.

(3) The flat-lying intrusions of the Trotternish sill complex intruded into Jurassic sediments have restricted $\delta^{34}S$ signatures of −5‰ to 0‰ (with one outlier of −10.8‰).

(4) The late vertical Robustan dykes cross-cutting the same Jurassic units have much lighter $\delta^{34}S$ ranging from −30‰ to −2‰.

Thus the data show that the potential contaminants of the British Palaeogene Igneous Province intrusive rocks on Skye have distinct S-isotope signatures, and our study has identified differences in S-isotope signature between different styles of intrusion. This provides insights into the sources of S, including local mantle and crustal signatures, and to shed light on models for emplacement and contamination in these intrusive rocks. These aspects are explored in detail below.

What is the value of the local mantle S-isotope signature in the British Palaeogene Igneous Province?

Several studies of the sulphur isotopic composition of oceanic basalts have previously been conducted (Kusakabe *et al*. 1990; Alt *et al*. 1993; Labidi *et al*. 2012). Most recently, the reappraisal of mid-ocean ridge basalt (MORB) $\delta^{34}S$ by Labidi *et al*. (2012) indicated that the mantle has a mean value around −1 ± 0.5‰. The sulphur content of such basalts is usually coupled with Fe, Ni and Cu, and is either found within sulphides or dissolved in the silicate melt. At magmatic temperatures, fractionation between the dissolved and segregated sulphide fractions of these basalts would be negligible and the bulk system reduced (Ohmoto & Rye 1979; Labidi *et al*. 2012). $\delta^{34}S$ of MORB and primary plume-derived magmas can thus be anticipated to broadly represent the $\delta^{34}S$ of the local mantle, particularly for primitive high-MgO magmatic rocks, where sulphur exsolution is assumed to be minimal, and contamination en route from the mantle likely to be limited (e.g. Iceland).

S-isotope analysis of Icelandic basalts show $\delta^{34}S$ from −2.0‰ to +0.4‰, with a mean of −0.8‰ (Torssander 1989). Both tholeiitic and alkaline basalts displayed similar isotopic compositions, although intermediate and acid rocks extend to heavier $\delta^{34}S$, up to +4.2‰. For the Icelandic alkaline and tholeiitic samples of Torssander (1989), the homogeneity of the $\delta^{34}S$ distribution provides strong evidence that the sulphur isotopic composition of the parental magmas had not changed significantly from the mantle source to crustal emplacement.

The mean $\delta^{34}S$ of the Trotternish Sills (excluding one anomalously light sample, SK102) is −2.3 ± 1.5‰, which is comparable with the signature of basalts from the Iceland plume (Torssander 1989) and MORB (Labidi *et al*. 2012), although the range of sulphur isotopic compositions is somewhat larger. Therefore we have confidence that the picritic Trotternish Sill Complex is representative of the mantle S-isotopic signature of the plume in this portion of the North Atlantic and British Palaeogene igneous provinces.

Crustal sulphur contamination in dykes from southern Skye

The sulphur isotopic composition and sulphur concentration for the basaltic Robustan dykes (SK127, SK129 and SK131) indicate that the magmas that formed these intrusions were contaminated by crustally derived sulphur with an isotopically light $\delta^{34}S$ signature. Assuming contamination is dominated by the Jurassic rocks a simple binary mixing model may be used, as follows:

$$\delta^{34}S_{mix} = \frac{\delta^{34}S_C X_C f + \delta^{34}S_M X_M (1-f)}{X_C f + X_M (1-f)} \quad (1)$$

where $\delta^{34}S_{mix}$ is the isotopic composition of the contaminated magma, $\delta^{34}S_M$ and $\delta^{34}S_C$ are the isotopic composition of the uncontaminated magma and contaminating sediment respectively, X_M and X_C are the concentration of sulphur in the uncontaminated magma and contaminating sediment respectively, and

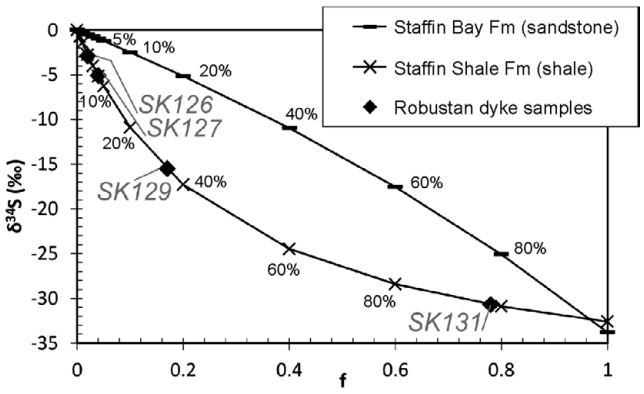

Fig. 7. Simple binary mixing model between a mantle melt (starting $\delta^{34}S = 0.0‰$, 250 ppm S) end-member, and a contaminating end-member of either Staffin Bay Formation sandstone, sample SK53 ($\delta^{34}S = -33.8‰$, <180 ppm S) or Staffin Shale Formation shale unit, sample SK50 ($\delta^{34}S = -32.6‰$, 1130 ppm S). Overlain on the plot are basalt dyke samples SK126, SK127, SK129 and SK131, with estimates of f (mass fraction of S from the contaminating end-member) for each sample.

f is the fractional abundance of the contaminant mixing with the magma.

Figure 7 shows a simple binary mixing model for $\delta^{34}S$ between an uncontaminated mantle melt and Jurassic sediments (SK50 and SK53). Assuming the $\delta^{34}S$ of the contaminant is similar to that of siltstone SK50, for dyke samples SK126 and SK127 between 2% and 4% input from the sediment S reservoir would account for the measured $\delta^{34}S$ in these dykes; whereas for SK129 ($\delta^{34}S = -15.5‰$) 17% contamination is required.

For sample SK131, the $\delta^{34}S$ of the contaminated dyke is calculable by accounting for 78% of the sulphur isotopic signature as coming from a contaminant (e.g. SK50). Sample SK131 was taken from a 30 cm wide basalt dyke. Although the field evidence, and whole-rock major and trace element geochemistry indicate that it is likely to be related to the other dyke samples from this area (with the exception of the basalt trachyandesite SK130), the S concentration of this dyke is not representative of the parental magma composition that fed the other Robustan dykes and intruded through neighbouring conduits. Local sulphur concentration could probably be extremely variable in the dykes, particularly if physical entrainment of crustal material is considered. Further, the sulphur concentration within the Jurassic sediments is extremely variable (e.g. sandstone v. pyrite nodule rich shale). Therefore, as the dykes were intruded through the Jurassic sediment package, they could have experienced contamination by each S-rich horizon in turn as the dyke intruded upwards.

Although we cannot eliminate the possibility of multi-component progressive contamination having taken place in the parental magmas of the dykes during ascent, we can use a mass-balance calculation to interpret the maximum contamination scenario. Assuming an initial concentration of 250 ppm sulphur in the parental basaltic magma (based on primitive mantle concentrations; McDonough & Sun 1995) for a volume of 1 m^3 of magma in a 1 m × 1 m × 1 m conduit with a 10 cm wide baked margin in the wall rocks either side (equivalent to 0.2 m^3 wall rock volume and based on visible field evidence) the concentration of sulphur in the wall rock would need to be *c*. 7.6 wt%, assuming a density of 3000 and 2600 kg m^{-3} for the basalt and shale respectively. This concentration is considerably higher than that measured in SK50 (1130 ppm). Assuming that the entire sedimentary S budget is accommodated within pyrite, this is equivalent to a shale containing 14% pyrite. Given that pyrite nodules are recorded within the Jurassic sediment pile of the Hebrides Basin, with 27.7 wt% S (e.g. sample AN71; Table 1) this is a feasible composition for the contaminant of SK131. Thus, our model can readily accommodate the observed dyke S concentrations and $\delta^{34}S$ if the high variability of S concentration in Jurassic shales and ironstones is taken into consideration. Dyke SK131 could have intruded through an isotopically light, pyrite-rich portion of the sedimentary pile with unusually higher S concentrations than the surrounding shales, thus dramatically reducing the volume of country rock required to be contaminating the magma conduit and accounting for the S-signature of the dyke.

Contrasting S-isotope signatures of sills and dykes on Skye

This study has presented two examples of high-level forms of intrusion from the British Palaeogene Igneous Province and shows that the dykes have incorporated substantial proportions of Jurassic S in both study areas on the Strathaird and Trotternish peninsulas (e.g. Lealt Quarry). In stark contrast, the sills of the Trotternish Sill Complex display limited sedimentary S contamination, even at the chilled sill margins. Therefore we have a dichotomy: crustally derived sulphur (with a characteristically light isotopic signature) is widely available in high concentrations within the country rocks of both areas, yet other factors appear to control whether or not this is mobilized or preserved in the local magmatic intrusions.

The possibility of post-magmatic sulphur mobility must be considered: is the sulphur signature observed in the dykes a feature of contamination during the magmatic event, or has this been imparted post-emplacement via *in situ* bacterial reduction in the basalts themselves, within fractures, or by low-temperature fluid remobilization? At Strathaird, the dykes are volumetrically small, and surrounded by isotopically light sulphur-bearing sediments. It is plausible that post-emplacement fluids could have circulated through these sediments and through the dykes, imparting the sedimentary $\delta^{34}S$ in this manner. However, textural diagnosis for the timing of sulphide mineral formation might be a better indicator. Where present, pyrite forms subhedral crystals up to 2 mm in diameter, typically within 20 cm of the dyke margin, and less common at dyke centres, although as highlighted above, this has not precluded the light whole-rock $\delta^{34}S$ signature from penetrating the dyke centres. As far as can be determined, there are no veinlets or stringers observed connecting these. In hand specimens, there is no correlation between the presence of oxidized fractures and pyrite, and oxidized or weathered material along with any vugs or amygdales was deliberately removed from the sample before sulphur extraction and analysis. Surface contamination from overlying peat bogs is a feature of the geography of both the dyke and sill areas, and therefore is unlikely to be a realistic modern source of S to one and not the other. Therefore at Strathaird, there is no reasonable evidence to presume that the sulphide signature is not a 'primary' feature.

Lastly, we can demonstrate physical evidence of high-level crustal contamination by sedimentary rocks taking place in British Palaeogene Igneous Province magmatic intrusions. The vertical basalt dyke at Lealt Quarry, Trotternish Peninsula, is observed in outcrop intruding through the horizontal picritic Trotternish Sills (Fig. 3a). At 50–80 m below this quarry, the sills overlie the Jurassic Lealt Shale Formation and it is assumed that the vertical basalt dyke extends through the sills and into the sedimentary pile below it. Field evidence of contamination comes from the centimetre-scale mudrock xenoliths entrained and preserved at the dyke margin (Fig. 3b–d). Pyrite crystals (up to several millimetres in diameter) nucleate within the basalt at the xenolith margins and the xenoliths themselves contain minor pyrite (mostly at the xenolith margins). The $\delta^{34}S$ of Trotternish Sills at Lealt Quarry are −2.2‰ and −1.7‰ (SK90 and SK92). Critically, this demonstrates that it

would not be possible to impart the light sulphur isotopic signature observed in the dyke from sulphur present in the host picritic sills. The mudrock xenoliths, although baked and with no characteristically distinguishing features, are undoubtedly from the Jurassic strata, possibly the Lealt Shale Formation or similar lithology, below the current level of exposure. The $\delta^{34}S$ of pyrite within the dyke at its margin is −7.5‰, whereas the whole-rock sulphur signature of the dyke centre is −6.5‰. The whole-rock sulphur signature of a mudrock xenolith is −15.4‰, suggesting that the light $\delta^{34}S$ of the dyke has been imparted from Jurassic mudrocks during dyke intrusion and ascent, and involved their physical attrition and brecciation. Accordingly, the intact wall rocks to the dyke were baked and chemically interacted with the intruding magma. This is analogous to the dykes on the Strathaird Peninsula, although xenoliths were not observed here, and is in complete contrast to the Trotternish Sills surrounding this dyke exposure.

Mass-independent sulphur diffusion profiles between the Platreef of the Bushveld Complex and footwall country rocks showed that the $\Delta^{33}S$ isotopic ratio is particularly sensitive to wall rock sulphur interaction (Penniston-Dorland *et al*. 2008). For example, the $\Delta^{33}S$ profile indicates enrichment of S at the Platreef footwall contact via back diffusion controlled by fluids emanating from the cooling and crystallizing magma. This process appears to be limited to 5 m inside the igneous contact; however, the diffusive and advective distances into the country rocks range from 6 to 9 m and 16 to 27 m respectively (Penniston-Dorland *et al*. 2008). In the Lealt Quarry dyke, it is unsurprising therefore that we observe the margins of the dyke to have a stronger sulphur contamination signature than at the centre, as this is where most magma–sediment interaction and element transfer was taking place during intrusion. Further, we demonstrate that it is highly unlikely that the sulphur isotopic signature of the dyke has been imparted post-emplacement by low-temperature fluids from the immediately surrounding host rocks, as the host rocks are picrite sills with a 'magmatic' $\delta^{34}S$ and are therefore not isotopically light enough to impart the $\delta^{34}S$ found in the basalt dyke.

We have established that the strongly negative $\delta^{34}S$ observed in the Skye dykes is a characteristic feature of the magmatic intrusions, inherited from Jurassic sedimentary pyrite with a bacteriogenic $\delta^{34}S$ signature, during the magmatic stage. The question arises, why is this signature so rare or absent in the Trotternish Sills? Is there an intrinsic difference between the sills and dykes and their capacity for local, high-level crustal contamination? After all, the sills and the dykes intrude through the same package of sediments on the Strathaird Peninsula as they do on the Trotternish Peninsula. And if contamination is taking place, is it wholesale melting–contamination (with inputs of all elements within the sediment being mixed with the magma), or is there preferential mobilization of only the most volatile elements such as sulphur?

The effect of emplacement mechanism on the crustal contamination signature

During intrusion, many mechanisms can control the upwards movement of magmas through the crust. These include zone melting, penetrative intrusion and stoping (Oxburgh *et al*. 1984). The physical method by which a magma body is emplaced could affect the degree of contamination that results. For example, the 'assimilability' of a country rock xenolith entrained in a magma depends on the size of that xenolith, viscous flow (Sachs & Stange 1993), and the mineralogical composition and melting temperature of the xenolith. In addition, the hydration and temperature of the entraining magma will also be a factor. It has been demonstrated that high-Mg basaltic magmas can ascend turbulently if they have a sufficiently high flow rate and conduit width (Campbell 1985; Huppert & Sparks 1985), delaying the formation of chilled margins and bringing hot magma into direct contact with country rocks for longer periods of time. Huppert and Sparks (1985) proposed that maximum contamination can occur in dykes which are at the minimum width for fully turbulent flow (*c*. 3 m) and evidence of turbulent flow in a basalt conduit has previously been described on the Isle of Mull (Kille *et al*. 1986).

The Jurassic mudrocks of the Hebrides Basin will predominantly comprise clay minerals and micas, with variable trace element compositions rich in Al, Si, Fe, Mg and Ti. Early stage melting of micaceous xenoliths has been shown to occur as an active melt zone at the xenolith rim, depleted in Al_2O_3 and enriched in CaO, MgO and TiO_2 relative to the bulk composition of the xenolith (Shaw 2009). Trace element mobility (e.g. large ion lithophile elements) will also be affected by the water content of this partial melt. We have tried to relate changes in Skye dyke whole-rock geochemistry with $\delta^{34}S$ but cannot resolve any correlation between dyke trace element composition and S isotopes. This is possibly because magma compositions were already significantly contaminated by deeper crustal silicic rocks (e.g. Moine and Lewisian basement), or may be due to variations in the original magma compositions (i.e. magma batches) such that trace element variation resulting from later input of Jurassic micaceous material would be masked. In addition, although field relations and hand specimens in our study provide good evidence for mudrock baking, *in situ* anatexis of these crustal rocks is not observed. This is in contrast to millimetre-scale veinlets of anatectic melt a few centimetres from a sill–shale contact (sill is 3 m wide) at Elgol, Skye (Yallup *et al*. 2013).

Sulphur and carbon will be mobilized, even without the need for partial melting *senso stricto* (therefore decoupling the trace element geochemistry), and transported as oxidized volatiles released from the baking of the xenolith and/or sedimentary wall rock. Evidence from mudrocks in contact with the Cuillin igneous centre on the Isle of Skye suggests that carbon can remain within these wall rocks despite severe baking and the high temperatures of the intrusion (Lindgren & Parnell 2006). However, that Cuillin study did not investigate the preservation of sulphur. The thermal effect of the Cuillin Complex was previously recognized as highly localized, using organic geochemical molecular maturity parameters (Thrasher 1992). Similarly, this localized thermal alteration has been found to be the case in limestone beds underlying the Trotternish Sills at Staffin Bay (Lefort *et al*. 2012). Nevertheless, sediments underlying sills at Duntulm show a more developed contact metamorphic sequence, including grossular garnet and pyroxene (contact metamorphism) and low-temperature alteration in microfractures containing clays (Kemp *et al*. 2005).

A doleritic sill at Elgol (southern Skye) that intruded through the Middle Jurassic Cullaidh Shale formation demonstrates that both sulphur and carbon may be baked out of sediments in this setting, up to 80 cm from the sill–sediment contact (Yallup *et al*. 2013). We suggest that a similar amount of sulphur assimilation took place during the intrusion of the Trotternish Sill Complex (scaled to the thicker, and presumably long-lived, sill complex). Yallup *et al*. (2013) also demonstrated that $\delta^{34}S$ became lighter towards the sediment–sill contact, and suggested that this is due to loss of ^{34}S-enriched SO_2 gas during sediment baking. We cannot demonstrate this feature in the Jurassic sediments at the base Trotternish sills because of the extremely low concentration of sulphur remaining in these rocks (they are almost devoid of S), which is probably due to substantial baking (and complete loss) of the sedimentary volatile budget.

On a global scale, the intrusion of sills (as part of large igneous provinces) into thick organic-rich sedimentary basins has been investigated by Svensen and co-workers. For example, hydrothermal vents originating from the base of sills have been identified in the Karoo Basin of South Africa (Svensen *et al*. 2006, 2007),

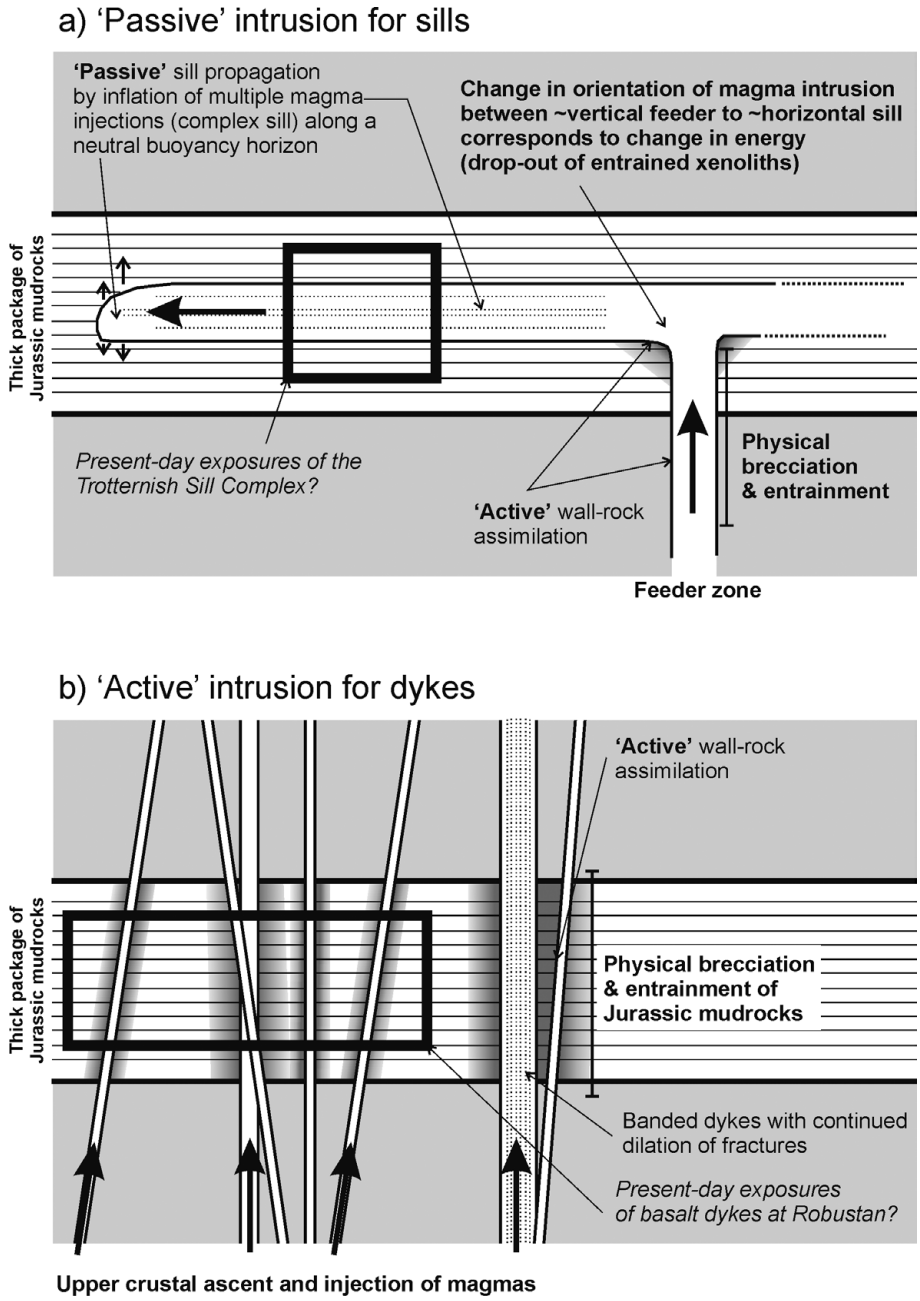

Fig. 8. (**a**) Passive intrusion of magmas forming sills: whereas the approximately vertically oriented feeder zone (or zones) is likely to actively assimilate and become contaminated by wall rocks during magma ascent, once the magma reaches a ductile horizon or zone of neutral buoyancy (spreading out horizontally) it is emplaced in a 'passive' environment of inflation. In this 'passive' setting, little physical attrition of wall rocks will occur so that little or no crustal S-isotope signature is imparted. (**b**) Active intrusion of magmas forming dykes: the approximately vertical and high-energy intrusion of magmas into upper-crustal levels forming dykes (e.g. at Lealt Quarry or Robustan) causes physical attrition or brecciation of wall rocks. This higher energy (or 'active') mechanism of emplacement leads to the entrainment of xenoliths (via wall rock attrition) and chemically leaches wall rocks of volatiles (S), imparting a crustal S-isotopic signature. In both cases (**a**) and (**b**), the contamination signature is inferred to be a local effect (magmas have transported the signature on a maximum scale of hundreds of metres).

Siberian Traps (Svensen *et al*. 2009) and Vøring Basin offshore Norway (Svensen *et al*. 2004; Planke *et al*. 2005). These form when large volumes of volatiles (C, S, H_2O) are baked out of sediments into which magmas have been intruded, and represent significant input of greenhouse gases into the atmosphere at a time coincident with global warming events and/or mass extinctions (e.g. Aarnes *et al*. 2010, 2011; Svensen *et al*. 2012, and references therein). Most of the aforementioned studies were concerned with the input of C or C-based gases, and did not fully investigate fluxing of S. Nonetheless, in this study we demonstrate the decoupled mobility of S from other trace elements, and highlight the requirement for future investigations into the relative mobilities of C and S (SO_2 is also an important greenhouse gas).

As magma ascends between clay-poor and clay-rich horizons, the amount of water and volatiles released will vary, with volatile-rich shales expected to chemically perpetuate the contamination process. Furthermore, the mechanical properties of a shale horizon may actively promote magma penetration. At shallow depths, over-pressured shale units can act as 'ductile horizons', permitting sill formation below the expected level of neutral buoyancy, leading to sill inflation and fracturing of the country rock. This has been documented in the North Atlantic Igneous Province in the Judd Basin, where Palaeogene magmas have intruded through a thick sequence of Jurassic–Palaeocene sediments, forming saucer-shaped sills (Thomson & Schofield 2008). It is possible that a similar mechanism of intrusion was in operation during formation of the Trotternish Sill Complex on Skye (Fig. 8a). We suggest that this entailed a comparatively 'passive' (i.e. predominantly non-brittle) emplacement mechanism for the magma, such that limited brecciation and entrainment of Jurassic country rock material took place. Where sediment–magma interaction did take place, probably at the chilled base of the sill complex, and in the vicinity of within-sill rafts of Jurassic sediments up to 10 m in thickness (Gibson & Jones 1991) the sediments became so baked, via contact metamorphism, that volatiles such as S and H_2O appear to have been entirely expelled. Many of the sills formed as a result of multiple injections, therefore magma flowing through the centre of the sill complex (i.e. from later injections) would have been effectively isolated from contamination effects in the approximately horizontal sill conduit itself (see Fig. 8a).

The large magma volume represented by the sill complex, and sustained magma throughput (at least in comparison with single basaltic dykes), could have effectively 'diluted' any crustal sulphur, thereby resulting in a limited change in sulphur concentration and/or $\delta^{34}S$ signature in the magma body. This is potentially analogous to conduit settings in Noril'sk, where sulphides that initially evolved following S-saturation became flushed out (Brügmann *et al*. 1993; Lightfoot & Keays 2005). Further, Cu/Pd, S-isotope and S/Se evidence from the sill-like intrusions of the Platreef (Bushveld Complex) suggests that S contamination from crustal rocks occurred early and deeper in the plumbing system below the Platreef (McDonald & Holwell 2007; McDonald *et al*. 2009; Sharman *et al*. 2013). These sulphides were transported away from this deeper zone during renewed or continued magma batch injections and ultimately emplaced in the Platreef itself (Ihlenfeld & Keays 2011). At Trotternish, prior contamination by deeper crustal material during fractionation is demonstrable through other isotope systems (e.g. Sr, Nd and Pb; Gibson 1990), and we suggest that contamination continued throughout the ascent of the sill complex's parental magmas. However, it is plausible that the change in the emplacement mechanism, owing to the change in orientation (i.e. from vertical ascent to horizontal emplacement) or rheology of the country rocks (i.e. brittle v. non-brittle deformation), would have significant implications for the conduit shape (Schofield *et al*. 2012) and degree of magma contamination, and, crucially, influenced element mobility during chemical reaction (Fig. 8a).

By contrast, the vertical dykes on Skye show widespread and exceptional degrees of sedimentary sulphur contamination. As mentioned above, physical brecciation and entrainment of Jurassic mudrocks is observed, and we suggest that the strong crustal chemical 'interaction' of the dykes (as demonstrated by the correlation between sulphur concentration and $\delta^{34}S$; Fig. 4b) is directly related to the magma emplacement mechanism (Fig. 8b). These narrow magma conduits, with comparatively limited magma volume, cooled more rapidly than the sills (as shown by their finer crystalline texture), evidently freezing in the local sulphur contamination signature. Dynamic mixing of magmas between the margins and centre of single dykes has taken place, thereby imparting the marginal contamination $\delta^{34}S$ signature to the dyke centre prior to crystallization; however, this process did not completely equilibrate the crustal sulphur input, so that measurable differences in $\delta^{34}S$ of up to 1‰ are observed between margins and centres of a 2 m wide dyke. A maximum degree of contamination probably occurred within the initial intrusive pulse of a dyke into any one given sedimentary horizon, with later pulses of magma along that conduit and through the dyke becoming progressively shielded from further contamination. Thus the mechanism of contamination in vertical dykes is probably complicated by multiple injections of magma, forming complex dykes (Fig. 8b). However, most of the examples sampled during this study do not display zoning or banding (with the exception of the dyke at Lealt Quarry), and therefore probably represent only a single magma pulse.

Crustal sulphur sources and contamination potential for Hebridean Scotland and the British Palaeogene Igneous Province

Identifying the crustal contaminants likely to be responsible for inducing S-saturation in ascending magmas is a key factor in pinpointing when and where immiscible sulphides and orthomagmatic Ni–Cu–PGE mineralization might have occurred. Therefore we have evaluated the S-isotopic signature of various potential S-bearing contaminants on a more regional scale for the British Palaeogene Igneous Province and Isle of Skye.

Apart from the Jurassic sedimentary rocks discussed so far, other upper-crustal sedimentary formations could also be contributors to the sulphur regime. For example, members of the Sleat and Torridon Groups present along the Sleat Peninsula on Skye, and on the Isle of Rum (Fig. 6, Table 1), irrespective of lithology and location, have positive $\delta^{34}S$ signatures, ranging +1.4‰ to +4.7‰. The Kinloch Formation mudstone had the highest $\delta^{34}S$ value of +4.7‰ (Fig. 6). Although it is possible that British Palaeogene Igneous Province magmas could be contaminated by Mesoproterozoic sediments, it is very unlikely that this material produced the light $\delta^{34}S$ signature seen in the sills and particularly the dykes of Skye. This is in contrast to the $\delta^{34}S$ results of certain members of the Stoer Group from the far NW Scottish mainland at Stoer Point, where values less than −30‰ are recorded (Parnell *et al*. 2010). If this material is widely present in the crust below the Isle of Skye, it is possible that the sulphur isotopic signatures of some of the British Palaeogene Igneous Province magma bodies presented here could have been contaminated by this Stoer Group material. However, Parnell *et al*. (2010) highlighted the patchy nature of this light S-isotope signature, with bacterial sulphate reduction constrained within small continental water bodies, the relicts of which are laterally discontinuous along strike. More directly, there is no surface exposure of the Stoer Group extending as far south as the Isle of Skye; only the equivalent Sleat Group is observed in this British Palaeogene Igneous Province area, and, as discussed above, analysis of this material indicates that its S-isotope signature is significantly heavier. Therefore the combination of the extremely heterogeneous sulphur isotope signature, and unconstrained subterranean extent of the Stoer Group, and other Torridonian sediments, makes this an unlikely candidate to explain the uniformly light $\delta^{34}S$ of the dykes and sills on Skye.

There is ample evidence that deeper crustal contamination via assimilation–fractional crystallization (AFC) and assimilation during turbulent ascent (ATA) took place across the British Palaeogene Igneous Province, in large deep staging chamber settings or in narrower metre-scale magma conduits. Both Lewisian (granulite- and amphibolite-facies) and Moinian contaminants have been successfully shown to explain the Sr, Nd, and Pb isotopic heterogeneities observed in British Palaeogene Igneous Province magmas (e.g. Gibson 1990; Kerr 1995; Preston *et al*. 1998). In particular, Gibson (1990) demonstrated that the Trotternish Sill Complex underwent up to *c*. 20% mid- or lower-crustal contamination, prior to magma injection and emplacement. Thompson (1982) and Gibson (1990) used La/Nb ratios to constrain assimilation of Lewisian rocks by Palaeogene magmas, now preserved as dykes, sills and lavas. There is no correlation between La/Nb ratio and $\delta^{34}S$ for dykes included in this study. There is a very weak and inconclusive correlation between La/Nb ratio and $\delta^{34}S$ for sills ($r^2 = 0.31$). Lewisian gneisses have variable but low sulphur concentrations and $\delta^{34}S$ ranging from −1.4‰ to +1.2‰ (this study) and from −1.4‰ to +5.5‰ on the NW Scottish mainland (Lowry *et al*. 2005). Torridonian sediments measured in this study always have $\delta^{34}S >$ 0‰. Moine metapelites also have low or very low concentrations of sulphur, and where measurable have $\delta^{34}S$ of +2.5‰ (this study) and +3.4‰ to +4.6‰ in some psammites (Lowry 1991). Accordingly, Lowry *et al*. (2005) found that each crustal terrane across Scotland could be characterized by its dominant crustal units, reflected in the range of $\delta^{34}S$ for that region. In the Northern Highland Terrane (which includes Skye) complexities in the terrane-scale $\delta^{34}S$ were suggested as reflecting the thick North Atlantic Craton (i.e. Lewisian and Palaeoproterozoic metasediments of Loch Maree) underlying the upper-crustal sedimentary cover.

Our study shows that both the Moine and Lewisian deeper crustal materials are unrealistic sources for the consistent and characteristically light sulphur isotopic signature of the Skye dykes.

Therefore, we suggest that although deep crustal contamination of British Palaeogene Igneous Province magmas has taken place, the dominant $\delta^{34}S$ contamination signature observed in these magmas is the result of specific and localized upper-crustal contamination of readily fusible, organic-rich Jurassic shales and mudrocks. This has taken place in smaller vertical magma conduits, or where the mudrocks were in direct contact with British Palaeogene Igneous Province magmas, allowing for pervasive alteration, mobilization of volatiles and in some cases physical and chemical assimilation of these country rocks, modelled by a simple binary mixing scenario.

Implications for Ni–Cu–PGE orthomagmatic sulphide mineralization

Although not the sole forcing factor in the occurrence of S-saturation, significant literature points to the common association of crustal contamination with the development of orthomagmatic sulphide mineralization (e.g. Noril'sk–Talnakh Region (Ripley *et al*. 2003; Ripley & Li 2013); Duluth (Arcuri *et al*. 1998); Voisey's Bay (Ripley *et al*. 1999); Kambalda (Lesher & Burnham 2001); and others (see Naldrett 2004, 2011, and references therein)). A scenario in which crustal sulphur is available for magma contamination is therefore often an important factor in Ni–Cu–PGE exploration. A recent study of lavas by Hughes *et al*. (2015) has suggested that the Scottish sector of the British Palaeogene Igneous Province is one of the most fertile regions of the North Atlantic Igneous Province for Ni–Cu–PGE mineralization, in part owing to the widespread opportunities for shallow crustal contamination by S-rich sediments.

Interpreting sulphide metal tenors and whole-rock chalcophile element abundances of magmas in relation to their degree of crustal sulphur contamination (monitored here by $\delta^{34}S$) can be complicated by the formation of multiple generations of sulphide liquids (i.e. deeper in the magmatic plumbing system; e.g. Holwell *et al*. 2007) and the effects of prolonged interaction of sulphides with fresh silicate magma(s) (Campbell & Naldrett 1979). The ultramafic sills have a low Cu/Pd ratio (13300–46200) in comparison with most of the basaltic Robustan dykes (5590 and 167200); however, this ratio is still elevated above that of primitive mantle (*c*. 7000–8000 based on pyrolite; McDonough & Sun 1995), suggesting that sulphide saturation had probably already taken place prior to emplacement of the sills. The highly variable Cu/Pd ratio of the Robustan dykes is probably also recording one or more S-saturation events that occurred prior to dyke emplacement. However, because the dykes are demonstrably assimilating local crustal sulphur at the current erosion level, we can further inspect the response of the remaining low-abundance chalcophile elements to this secondary S-saturation event.

Broadly, dyke samples with the lightest crustal $\delta^{34}S$ signatures have the lowest Pd concentration (Fig. 5a) and highest Cu/Pd ratio (Fig. 5c). Pt, Pd and Au concentrations show the strongest response to localized crustal S contamination, and variations in Cu appear to be weaker (i.e. there are less variable concentrations) in this secondary S-saturation scenario. This causes a correspondingly 'delayed' spike in Cu/Pd ratio. In PGE mineralized settings (e.g. the Bushveld Complex) this feature is well documented for S-saturation in PGE reefs (Maier 2005, and references therein) as the partition coefficient of Pd into sulphide liquid is several orders of magnitude greater than that for Cu (Mungall *et al*. 2005; Mungall & Brenan 2014). However, in a setting where first-stage S-saturation has already occurred deeper in the system, the concentration of chalcophile elements (particularly Pd-group PGE) would be much lower in the remaining silicate magma that continued its ascent to the surface. Therefore the Cu/Pd ratio of that residual silicate magma would be much higher and more variable than that of a magma, which had undergone only one S-saturation event (as seen in the Trotternish Sills). From this secondary 'starting point' Cu/Pd ratio, a second-stage localized S-saturation event would lead to further fractionation of Pd from Cu (particularly for systems with low R-factors; the ratio of sulphide liquid to silicate magma), raising Cu/Pd ratio to even higher values (up to 167000 in sample SK131). Assuming sulphide liquids from the initial S-saturation event had not been entrained during continued magma ascent, the extreme variability in Cu/Pd ratio caused by this first S-saturation (deeper) would lead to an even more erratic nature for this parameter during the formation of later sulphide liquids (shallower). Thus, in the absence of entrained sulphide liquids, the detailed interpretation of chalcophile element ratios at or after secondary S-saturation events would be impractical.

The cause for this first-stage S-saturation event remains speculative; given the silicic basement underlying this region, it could have been due to the addition of SiO_2 to the magma (as well as fractional crystallization during magma ascent) such that S concentration at sulphide-saturation (SCSS) was lowered. Alternatively, it could have been triggered by addition of S deeper in the crust, but during this study we have shown that $\delta^{34}S$ of Moine, Torridonian and Lewisian rocks is within magmatic variation (0 ± 4‰) and therefore would not be detected by this method. However, we have also determined that S abundance in these lithologies is typically very low, and we question the likelihood of these rocks contributing enough S during deep crustal contamination to induce S-saturation.

Ultimately, the effects of multiple S-saturation events might be further investigated by analysis of the S/Se ratio of sulphide minerals (e.g. Ihlenfeld & Keays 2011). In addition, the earlier S-saturation of magmas would probably preclude significant orthomagmatic Ni–Cu–PGE mineralization in higher portions of a magmatic province. However, by identifying the physical and structural factors controlling the ability of an ascending magma to assimilate crustal sulphur in a conduit, we can ascertain the locations within a magmatic plumbing system (deep or shallow) where S-saturation is likely to have taken place, leading to mineralization.

Finally, the small (±1.4‰) and non-systematic variation observed between $\delta^{34}S$ of sulphide minerals (in this case, pyrite) compared with whole-rock values is acceptable for use in identifying the occurrence of contamination of magmas by crustally derived sulphur. The observed maximum procedural-induced isotopic shift is very small in comparison with the isotopic shift caused by crustal contamination and the natural $\delta^{34}S$ of the country rock samples. However, this is dependent on the crustal sulphur source having a characteristic $\delta^{34}S$ signature (either light or heavy), and being statistically different from the typical 'mantle' signature. Therefore the whole-rock CRS method of sample preparation for $\delta^{34}S$ analysis (as used in this study) is suitable for identifying areas of potential sulphur saturation in mantle-derived magmas contaminated by crustal sulphur. This contributes to a rapid and flexible exploration tool for orthomagmatic Ni–Cu–PGE sulphide deposits, applicable even to samples with non-visible sulphide mineralization, as it identifies crustal sulphur contamination of whole-rock magmatic samples, assuming that there is a significant difference between the sedimentary and mantle $\delta^{34}S$ composition. This method offers the opportunity to focus on areas of increased crustal S contamination, even in relatively S-poor rocks.

Conclusion

(1) The $\delta^{34}S$ range for the Palaeogene alkali picritic Trotternish Sill Complex (+0.1‰ to −4.9‰; mean $= -2.3 \pm 1.5$‰) reflects the dominance of mantle-derived sulphur, consistent with that found in other Icelandic mantle plume-derived magmas.

(2) In contrast, the observed $\delta^{34}S$ range for the Palaeogene basaltic Robustan dykes is −2.3‰ to −30.7‰. Sulphur isotope

evidence for contamination is present throughout the full widths of these dykes: margins and centres alike.

(3) There appears to be a fundamental geological control on the degree of crustal contamination of magma bodies, depending of the mechanism (orientation and energy) by which that magma intruded. In spite of similar country rocks characterized by light $\delta^{34}S$ (> −33.8‰), there is a distinct difference in the S contamination pattern between a flat-lying concordant and thicker magma conduit (as represented by the 10–100 m scale Trotternish Sill Complex, $\delta^{34}S$ from −4.9‰ to +0.1‰ with one outlier of −10.8‰) and a vertically intruded discordant and narrow magma conduit (metre-scale basaltic Robustan dykes, $\delta^{34}S$ from −2.3‰ to −30.7‰).

(4) Turbulent flow within narrow magma conduits emplaced discordantly to sediments maximizes contamination potential, particularly of volatile and highly mobile elements (such as S) in a high surface-to-volume scenario, whereas passively emplaced, wide conduits emplaced concordantly to the sediments undergo comparatively little crustal sulphur contamination. This mechanical control may act in addition to other known controls on contamination such as the temperature and flux rate of magma in a conduit system.

(5) Despite the absence of sulphide minerals, a S-saturation event prior to dyke emplacement may be identified using Cu/Pd ratio. Given the high concentration of S in these dykes, and their strong $\delta^{34}S$ crustal contamination signature, S-saturation causing this extreme variability in Cu/Pd ratio must have been imparted before dyke emplacement and therefore at a deeper crustal level. This suggests that Ni–Cu–PGE mineralization may exist below current exposure levels. However, the trigger for this previous S-saturation remains unresolved.

(6) Where sulphide minerals are either too rare or too small to separate, use of whole-rock sulphur extraction to analyse $\delta^{34}S$ in samples can reveal S contamination. We suggest that this technique offers a suitable and rapid method that can be used as an aid in exploration of orthomagmatic Ni–Cu–PGE mineralization.

Acknowledgements and Funding

Sulphur isotope analysis was undertaken at the Scottish Universities Environment Research Centre (SUERC) and funded by an NERC Isotope Geosciences Facilities Steering Committee grant (IP-1356-1112). H.S.R.H. would like to acknowledge the financial support of the Natural Environment Research Council (NERC) for funding this work (studentship NE/J50029X/1) and open access publication. A.J.B. is funded by NERC funding of the Isotope Community Support Facility at SUERC. The paper benefited from discussions with B. Manton, G. Steed and A. Kerr. S. Gibson and B. Bingen are thanked for their thorough and constructive reviews.

Scientific editing by Bernard Bingen

References

Aarnes, I., Svensen, H., Connolloy, J.A.D. & Podladchikov, Y.Y. 2010. How contact metamorphism can trigger global climate changes: Modeling gas generation around igneous sills in sedimentary basins. *Geochimica et Cosmochimica Acta*, **74**, 7179–7195.

Aarnes, I., Svensen, H., Polteau, S. & Planke, S. 2011. Contact metamorphic devolatilization of shales in the Karoo Basin, South Africa, and the effects of multiple sill intrusions. *Chemical Geology*, **281**, 181–194.

Alt, J., Shanks, W. & Jackson, M. 1993. Cycling of sulphur in subduction zones: The geochemistry of sulphur in the Mariana Island Arc and back-arc trough. *Earth and Planetary Science Letters*, **119**, 477–494.

Arcuri, T., Ripley, E.M. & Hauck, S.A. 1998. Sulphur and oxygen isotope studies of the interaction between pelitic xenoliths and basaltic magma at the Babbitt and Serpentine Cu–Ni deposits, Duluth Complex, Minnesota. *Economic Geology*, **93**, 1063–1075.

Bell, B.R. & Williamson, I.T. 2002. Tertiary volcanism. *In*: Trewin, N.H., (ed.) *The Geology of Scotland*, 4th edn. Geological Society, London, 317–407.

Brügmann, G.E., Naldrett, A.J., Asif, M., Lightfoot, P., Gorbachev, N.S. & Fedorenko, V.A. 1993. Siderophile and chalcophile metals as tracers of the evolution of the Siberian Trap in the Noril'sk region, Russia. *Geochimica et Cosmochimica Acta*, **57**, 2001–2018.

Campbell, I.H. 1985. The difference between oceanic and continental tholeiites: A fluid dynamic explanation. *Contributions to Mineralogy and Petrology*, **91**, 37–43.

Campbell, I.H. & Naldrett, A.J. 1979. The influence of silicate:sulphide ratios on the geochemistry of magmatic sulphides. *Economic Geology*, **74**, 1503–1506.

Canfield, D.E. & Teske, A. 1996. Late Proterozoic rise in atmospheric oxygen concentration inferred from phylogenetic and sulphur-isotope studies. *Nature*, **382**, 127–132.

Canfield, D.E., Raiswell, R., Westrich, J.T., Reaves, C.M. & Berner, R.A. 1986. The use of chromium reduction in the analysis of reduced inorganic sulphur in sediments and shales. *Chemical Geology*, **54**, 149–155.

Emeleus, C.H. & Bell, B.R. 2005. *British Regional Geology: The Palaeogene Volcanic Districts of Scotland*. British Geological Survey, Nottingham.

Fisher, I. St I.J. & Hudson, J.D. 1987. Pyrite formation in Jurassic shales of contrasting biofacies. *In*: Brooks, J., & Fleet, A.J. (eds) *Marine Petroleum Source Rocks*. Geological Society, London, Special Publications, **26**, 69–78, http://dx.doi.org/10.1144/GSL.SP.1987.026.01.04.

Fyfe, J.A., Long, D. & Evans, D. (1993). *The geology of the Malin-Hebrides sea area*. British Geological Survey, United Kingdom Offshore Regional Report.

Gibb, F.G.F. & Gibson, S.A. 1989. The Little Minch Sill Complex. *Scottish Journal of Geology*, **25**, 367–370, http://dx.doi.org/10.1144/sjg25030367.

Gibson, S.A. 1990. The geochemistry of the Trotternish sills, Isle of Skye: Crustal contamination in the British Tertiary Volcanic Province. *Journal of the Geological Society, London*, **147**, 1071–1081, http://dx.doi.org/10.1144/gsjgs.147.6.1071.

Gibson, S.A. & Jones, A.P. 1991. Igneous stratigraphy and internal structure of the Little Minch Sill Complex, Trotternish Peninsula, northern Skye, Scotland. *Geological Magazine*, **128**, 51–66.

Hall, G.E.M., Pelchat, J.-C. & Loop, J. 1988. Separation and recovery of various sulphur species in sedimentary rocks for stable sulphur isotopic determination. *Chemical Geology*, **67**, 35–45.

Harker, A. 1904. *The Tertiary Igneous Rocks of Skye. Memoir of the Geological Survey of Great Britain*. HMSO, Edinburgh.

Hesselbo, S.P. & Coe, A.L. 2000. Jurassic sequences of the Hebrides Basin, Isle of Skye, Scotland. *In*: Graham, J.R., & Ryan, A. (eds) *Field Trip Guidebook*. International Association of Sedimentologists, Dublin, 41–58.

Holwell, D.A., Boyce, A.J. & McDonald, I. 2007. Sulphur isotope variations within the Platreef Ni–Cu–PGE deposit: Genetic implications for the origin of sulphide mineralization. *Economic Geology*, **102**, 1091–1110.

Huber, H., Koeberl, C., McDonald, I. & Reimond, W.U. 2000. Use of γ–γ coincidence spectrometry in the geochemical study of diamictites from South Africa. *Journal of Radioanalytical and Nuclear Chemistry*, **244**, 603–607.

Hudson, J.D., Coleman, M.L., Barreiro, B.A. & Hollingworth, N.T.J. 2001. Septarian concretions from the Oxford Clay (Jurassic, England, UK): Involvement of original marine and multiple external pore fluids. *Sedimentology*, **48**, 507–531.

Hughes, H.S.R., McDonald, I. & Kerr, A.C. 2015. Platinum group element signatures in the North Atlantic Igneous Province: Implications for mantle controls on metal budgets during continental breakup. *Lithos* (in press), http://doi.org.10.1016/j.lithos.2015.05.005.

Huppert, H.E. & Sparks, S.J. 1985. Cooling and contamination of mafic and ultramafic magmas during ascent through continental crust. *Earth and Planetary Science Letters*, **74**, 371–386.

Ihlenfeld, C. & Keays, R.R. 2011. Crustal contamination and PGE mineralization in the Platreef, Bushveld Complex, South Africa: Evidence for multiple contamination events and transport of magmatic sulphides. *Mineralium Deposita*, **46**, 813–832.

Kemp, S.J., Rochelle, C.A. & Merriman, R.J. 2005. Back-reacted saponite in Jurassic mudstones and limestones intruded by a Tertiary sill, Isle of Skye. *Clay Minerals*, **40**, 263–282.

Kent, R.W., Thomson, B.A., Skelhorn, R.R., Kerr, A.C., Norry, M.J. & Walsh, J.N. 1998. Emplacement of Hebridean Tertiary flood basalts: Evidence from an inflated pahoehoe lava flow on Mull, Scotland. *Journal of the Geological Society, London*, **155**, 599–607, http://dx.doi.org/10.1144/gsjgs.155.4.0599.

Kerr, A.C. 1995. The geochemistry of the Mull–Morvern lava succession, NW Scotland: An assessment of mantle sources during plume-related volcanism. *Chemical Geology*, **122**, 43–58.

Kille, I.C., Thompson, R.N., Morrison, M.A. & Thompson, R.F. 1986. Field evidence for turbulence during flow of basalt magma through conduits from southwest Mull. *Geological Magazine*, **123**, 693–697.

Kinnaird, T.C., Prave, A.R., Kirkland, C.L., Horstwood, M., Parrish, R. & Batchelor, R.A. 2007. The late Mesoproterozoic–early Neoproterozoic tectonostratigraphic evolution of NW Scotland: The Torridonian revisited. *Journal of the Geological Society, London*, **164**, 541–551, http://dx.doi.org/10.1144/0016-76492005-096.

Kusakabe, M., Mayeda, S. & Nakamura, E. 1990. S, O and Sr isotope systematics of active vent materials from the Mariana Back Arc Basin spreading axis at 18°N. *Earth and Planetary Science Letters*, **100**, 275–282.

Labidi, J., Cartigny, P., Birck, J.L., Assayag, N. & Bourrand, J.J. 2012. Determination of multiple sulphur isotopes in glasses: A reappraisal of the MORB $\delta^{34}S$. *Chemical Geology*, **334**, 189–198.

Lefort, A., Hautevelle, Y., Lathuiliere, B. & Huault, V. 2012. Molecular organic geochemistry of a proposed stratotype for the Oxfordian/Kimmeridgian boundary (Isle of Skye, Scotland). *Geological Magazine*, **149**, 857–874.

Lesher, C.E. & Burnham, O.M. 2001. Multicomponent elemental and isotopic mixing in Ni–Cu–(PGE) ores at Kambalda, Western Australia. *Canadian Mineralogist*, **39**, 421–446.

Lightfoot, P. & Keays, R.R. 2005. Siderophile and chalcophile metal variations in flood basalts from the Siberian Trap, Noril'sk Region: Implications for the origin of the Ni–Cu–PGE sulphide ores. *Economic Geology*, **100**, 439–462.

Lindgren, P. & Parnell, J. 2006. Rapid heating of carbonaceous matter by igneous intrusions in carbon-rich shale, Isle of Skye, Scotland: An analogue for heating of carbon in impact craters? *International Journal of Astrobiology*, **5**, 343–351.

Lowry, D. 1991. *The genesis of Late Caledonian granitoid-related mineralization in Northern Britain*. PhD thesis, University of St Andrews.

Lowry, D., Boyce, A.J., Fallick, A.E., Stephens, W.E. & Grassineau, N.V. 2005. Terrane and basement discrimination in northern Britain using sulphur isotopes and mineralogy of ore deposits. *In*: McDonald, I., Boyce, A.J., Butler, I.B., Herrington, R.J. & Polya, D.A. (eds) *Deposits and Earth Evolution*. Geological Society, London, Special Publications, **248**, 133–151, http://dx.doi.org/10.1144/GSL.SP.2005.248.01.07.

Maier, W.D. 2005. Platinum-group element (PGE) deposits and occurrences: Mineralization styles, genetic concepts, and exploration criteria. *Journal of African Earth Sciences*, **41**, 165–191.

McDonald, I. & Holwell, D.A. 2007. Distribution of platinum-group elements in the Platreef at Overysel, northern Bushveld Complex: A combined PGM and LA-ICP-MS study. *Contributions to Mineralogy and Petrology*, **154**, 171–190.

McDonald, I. & Viljoen, K.S. 2006. Platinum-group element geochemistry of mantle eclogites: A reconnaissance study of xenoliths from the Orapa kimberlite, Botswana. *Applied Earth Science*, **115**, 81–93.

McDonald, I., Holwell, D.A. & Wesley, B. 2009. Assessing the potential involvement of an early magma staging chamber in the generation of the Platreef Ni–Cu–PGE deposit in the northern limb of the Bushveld Complex: A pilot study of the Lower Zone Complex at Zwartfontein. *Applied Earth Science (Transactions, Institute of Mining and Metallurgy B)*, **118**, 5–20.

McDonough, W.F. & Sun, S.-S. 1995. The composition of the Earth. *Chemical Geology*, **120**, 223–253.

Morton, N. & Hudson, J.D. 1995. Field guide to the Jurassic of the Isles of Raasay and Skye, Inner Hebrides, NW Scotland. *In*: Taylor, P.D., (ed.) *Field Geology of the British Jurassic*. Geological Society, London, 209–280.

Mungall, J., Andrews, D.R.A., Cabri, L.J., Sylvester, P.J. & Tubrett, M. 2005. Partitioning of Cu, Ni, Au, and platinum-group elements between monosulphide solid solution and sulphide melt under controlled oxygen and sulphur fugacities. *Geochimica et Cosmochimica Acta*, **69**, 4349–4360.

Mungall, J.E. & Brenan, J.M. 2014. Partitioning of platinum-group elements and Au between sulphide liquid and basalt and the origins of mantle–crust fractionation of the chalcophile elements. *Geochimica et Cosmochimica Acta*, **125**, 265–289.

Naldrett, A.J. 2004. *Magmatic Sulphide Deposits: Geology, Geochemistry and Exploration*. Springer, Berlin.

Naldrett, A.J. 2011. Fundamentals of magmatic sulphide deposits. *In*: Li, C., & Ripley, E.M. (eds) *Magmatic Ni–Cu and PGE Deposits: Geology, Geochemistry, and Genesis*. Society of Economic Geologists, Reviews in Economic Geology, **17**, 1–51.

Newton, R.J., Bottrell, S.H., Dean, S.P., Hatfield, D. & Raiswell, R. 1995. An evaluation of the use of the chromous chloride reduction method for isotopic analyses of pyrite in rocks and sediment. *Chemical Geology*, **125**, 317–320.

Nielsen, J.K. & Hanken, N.-M. 2002. *Description of the Chromium Reduction Method for Extraction of Pyrite Sulphur*. University of Tromso.

Ohmoto, H. & Goldhaber, M.B. 1997. Sulphur and carbon isotopes. *In*: Barnes, H.L. (ed.) *Geochemistry of Hydrothermal Ore Deposits*, 3rd edn. Wiley, New York, 517–611.

Ohmoto, H. & Rye, R.O. 1979. Isotopes of sulphur and carbon. *In*: Barnes, H.L., (ed.) *Geochemistry of Hydrothermal Ore Deposits*. Wiley, New York, 509–567.

Oxburgh, E.R., McRae, T. & O'Hara, M.J. 1984. Physical constraints on magma contamination in the continental crust: An example, the Adamello Complex [and Discussion]. *Philosophical Transactions of the Royal Society, Series A*, **310**, 457–472.

Parnell, J., Boyce, A.J., Mark, D., Bowden, S. & Spinks, S. 2010. Early oxygenation of the terrestrial environment during the Mesoproterozoic. *Nature*, **468**, 290–293.

Parnell, J., Hole, M., Boyce, A.J., Spinks, S. & Bowden S. 2012. Heavy metal, sex and granites: Crustal differentiation and bioavailability in the mid-Proterozoic. *Geology*, **40**, 751–754.

Penniston-Dorland, S.C., Wing, B.A., Nex, P.A.M., Kinnaird, J.A., Farquhar, J., Brown, M. & Sharman, E.R. 2008. Multiple sulphur isotopes reveal a magmatic origin for the Platreef platinum group element deposit, *Bushveld Complex*, South Africa. *Geology*, **36**, 979–982.

Planke, S., Rassmussen, T., Rey, S.S. & Myklebust, R. 2005. Seismic characteristics and distribution of volcanic intrusions and hydrothermal vent complexes in the Vøring and Møre basins. *In*: Doré, T., & Vining, B. (eds) *Petroleum Geology: North-West Europe and Global Perspectives*. Geological Society, London, 833–844.

Platten, I.M. 2000. Incremental dilation of magma filled fractures: Evidence from dykes on the Isle of Skye, Scotland. *Journal of Structural Geology*, **22**, 1153–1164.

Preston, R.J., Bell, B.R. & Rogers, G. 1998. The Loch Scridain sill complex, Isle of Mull, Scotland: Fractional crystallization, assimilation, magma-mixing and crustal anatexis in sub-volcanic conduits. *Journal of Petrology*, **39**, 519–550.

Raiswell, R., Bottrell, S.H., Al-Biatty, H.J. & Tan, M.M. 1993. The influence of bottom water oxygenation and reactive iron content on sulphur incorporation into bitumens from Jurassic marine shales. *American Journal of Science*, **293**, 569–596.

Ripley, E.M. & Li, C. 2013. Sulphide saturation in mafic magmas: Is external sulphur required for magmatic Ni–Cu–(PGE) ore genesis? *Economic Geology*, **108**, 45–58.

Ripley, E.M., Park, Y.-R., Li, C. & Naldrett, A.J. 1999. Sulphur and oxygen isotopic evidence of country rock contamination in the Voisey's Bay Ni–Cu–Co deposit, Labrador, Canada. *Lithos*, **47**, 53–68.

Ripley, E.M., Lightfoot, P.C., Li, C. & Elswick, E.R. 2003. Sulphur isotopic studies of continental flood basalts in the Noril'sk region: Implications for the association between lavas and ore-bearing intrusions. *Geochimica et Cosmochimica Acta*, **67**, 2805–2817.

Robinson, B.W. & Kusakabe, M. 1975. Quantitative preparation of sulphur dioxide for $^{34}S/^{32}S$ analyses from sulphides by combustion with cuprous oxide. *Analytical Chemistry*, **47**, 1179–1181.

Sachs, P.M. & Stange, S. 1993. Fast assimilation of xenoliths in magmas. *Journal of Geophysical Research*, **98**, 19741.

Saunders, A.D., Fitton, J.G., Kerr, A.C., Norry, M.J. & Kent, R.W. 1997. The North Atlantic Igneous Province. *In*: Mahoney, J.J., & Coffin, M.F. (eds) *Large Igneous Provinces: Continental, Oceanic, and Planetary Flood Volcanism*. American Geophysical Union, Geophysical Monograph, **100**, 45–93.

Schofield, N.J., Brown, D.J., Magee, C. & Stevenson, C.T. 2012. Sill morphology and comparison of brittle and non-brittle emplacement mechanisms. *Journal of the Geological Society, London*, **169**, 127–141, http://dx.doi.org/10.1044/0016-76492011-078.

Sharman, E.R., Penniston-Dorland, S.C., Kinnaird, J.A., Nex, P.A.M., Brown, M. & Wing, B.A. 2013. Primary origin of marginal Ni–Cu–(PGE) mineralization in layered intrusions: $\delta^{33}S$ evidence from the Platreef, Bushveld, South Africa. *Economic Geology*, **108**, 365–377.

Shaw, C.S.J. 2009. Caught in the act—The first few hours of xenolith assimilation preserved in lavas of the Rockeskyllerkopf volcano, West Eifel, Germany. *Lithos*, **112**, 511–523.

Simkin, T. 1967. Flow differentiation in the picritic sills of north Skye. *In*: Wyllie, P.J., (ed.) Ultramafic and Related Rocks. Wiley, New York, 64–69.

Stewart, A.D. 2002. *The Later Proterozoic Torridonian Rocks of Scotland: Their Sedimentology, Geochemistry and Origin*. Geological Society, London.

Svensen, H., Planke, S., Malthe-Sørenssen, A., Jamtveit, B., Myklebust, R., Eidem, T.R. & Rey, S.S. 2004. Release of methane from a volcanic basin as a mechanism for initial Eocene global warming. *Nature*, **429**, 542–545.

Svensen, H., Jamtveit, B., Planke, S. & Chevallier, L. 2006. Structure and evolution of hydrothermal vent complexes in the Karoo Basin, South Africa. *Journal of the Geological Society, London*, **163**, 671–682, http://dx.doi.org/10.1044/1144-764905-037.

Svensen, H., Planke, S., Chevallier, L., Malthe-Sørenssen, A., Corfu, F. & Jamtveit, B. 2007. Hydrothermal venting of greenhouse gases triggering Early Jurassic global warming. *Earth and Planetary Science Letters*, **256**, 554–566.

Svensen, H., Planke, S., Polozov, A.G., Schidbauer, N., Corfu, F., Podladchikov, Y.Y. & Jamtveit, B. 2009. Siberian gas venting and the end-Permian environmental crisis. *Earth and Planetary Science Letters*, **277**, 490–500.

Svensen, H., Corfu, F., Polteau, S., Øyvind H. & Planke, S. 2012. Rapid magma emplacement in the Karoo Large Igneous Province. *Earth and Planetary Science Letters*, **325–326**, 1–9.

Thompson, R.N. 1982. Magmatism of the British Tertiary Volcanic Province. *Scottish Journal of Geology*, **18**, 49–107, http://dx.doi.org/10.1144/sjg18010049.

Thomson, K. & Schofield, N. 2008. Lithological and structural controls on the emplacement and morphology of sills in sedimentary basins. *In*: Thomson, K., & Petford, N. (eds) *Structure and Emplacement of High-level Magmatic Systems*. Geological Society, London, Special Publications, **302**, 31–44, http://dx.doi.org/10.1144/SP302.3.

Thrasher, J. 1992. Thermal effect of the Tertiary Cuillins Intrusive Complex in the Jurassic of the Hebrides: An organic geochemical study. *In*: Parnell, J., (ed.) *Basins on the Atlantic Seaboard: Petroleum Geology, Sedimentology and Basin Evolution*. Geological Society, London, 35–49.

Torssander, P. 1989. Sulphur isotope ratios of Icelandic rocks. *Contributions to Mineralogy and Petrology*, **102**, 18–23.

Tuttle, M.L., Goldhaber, M.B. & Williamson, D.L. 1986. An analytical scheme for determining forms of sulphur in oil shales and associated rocks. *Talanta*, **33**, 953–961.

Wagner, T., Boyce, A. & Fallick, A.E. 2002. Laser combustion analysis of $\delta^{34}S$ of sulfosalt minerals: Determination of the fractionation systematics and some crystal-chemical considerations. *Geochimica et Cosmochimica Acta*, **66**, 2855–2863.

Yallup, C., Edwards, M. & Turchyn, A.V. 2013. Sulphur degassing due to contact metamorphism during flood basalt eruptions. *Geochimica et Cosmochimica Acta*, **120**, 263–279.

Zhabina, N. & Volkov, I. 1978. A method of determination of various sulphur compounds in sea sediments and rocks. *In*: Krumbein, W.E. (ed) *Environmental biogeochemistry and geomicrobiology. Vol. 3: Methods, metals and assessment*. Ann Arbor Science Publications, Ann Arbor, MI, 735–746.